คอนจูเกต BODIPY-ซาลิไซลัลดีไฮด์โพรบเพื่อเป็นตัวรับรู้ไซยาไนด์ทางฟลูออเรสเซนต์และการเทียบสี

นายรังสฤษฏ์ สุคโต

วิทยานิพนธ์นี้เป็นส่วนหนึ่งของการศึกษาตามหลักสูตรปริญญาวิทยาศาสตรมหาบัณฑิต
สาขาวิชาปิโตรเคมีและวิทยาศาสตร์พอลิเมอร์
คณะวิทยาศาสตร์ จุฬาลงกรณ์มหาวิทยาลัย
ปีการศึกษา 2557

CONJUGATED BODIPY-SALICYLALDEHYDE PROBES AS FLUORESCENT AND COLORIMETRIC CYANIDE SENSORS

Mr. Rangsarit Sukato

A Thesis Submitted in Partial Fulfillment of the Requirements
for the Degree of Master of Science Program in Petrochemistry and Polymer Science
Faculty of Science
Chulalongkorn University
Academic Year 2014

Thesis Title	CONJUGATED BODIPY-SALICYLALDEHYDE PROBES AS FLUORESCENT AND COLORIMETRIC CYANIDE SENSORS
By	Mr. Rangsarit Sukato
Field of Study	Petrochemistry and Polymer Science
Thesis Advisor	Assistant Professor Sumrit Wacharasindhu, Ph.D.
Thesis Co-Advisor	Professor Mongkol Sukwattanasinitt, Ph.D.

Accepted by the Faculty of Science, Chulalongkorn University in Partial Fulfillment of the Requirements for the Master's Degree

.....Dean of the Faculty of Science
(Professor Supot Hannongbua, Dr.rer.nat.)

THESIS COMMITTEE

.....Chairman
(Assistant Professor Warinthorn Chavasiri, Ph.D.)

.....Thesis Advisor
(Assistant Professor Sumrit Wacharasindhu, Ph.D.)

.....Thesis Co-Advisor
(Professor Mongkol Sukwattanasinitt, Ph.D.)

.....Examiner
(Assistant Professor Nuanphun Chantarasiri, Ph.D.)

.....External Examiner
(Gamolwan Tumcharern, Ph.D.)

รังสฤษฏ์ สุคโต : คอนจูเกต BODIPY-ซาลิไซลัลดีไฮด์โพรบเพื่อเป็นตัวรับรู้ไซยาไนด์ทางฟลูออเรสเซนต์และการเทียบสี (CONJUGATED BODIPY-SALICYLALDEHYDE PROBES AS FLUORESCENT AND COLORIMETRIC CYANIDE SENSORS) อ.ที่ปรึกษาวิทยานิพนธ์หลัก: ผศ. ดร.สัมฤทธิ์ วัชรสินธุ์, อ.ที่ปรึกษาวิทยานิพนธ์ร่วม: ศ. ดร.มงคล สุขวัฒนาสินิทธิ์, 4 หน้า.

ในปัจจุบันมีแนวโน้มการออกแบบวิธีการตรวจวัดไซยาไนด์แบบจำเพาะเจาะจงที่สูงขึ้น เพราะไซยาไนด์นั้นเป็นหนึ่งในแอนไอออนที่อันตรายที่สุดต่อสุขภาพมนุษย์และสิ่งแวดล้อม ในที่นี้เราได้สังเคราะห์อนุพันธุ์ BODIPY ชื่อ GSB และ RSB ที่ใช้ตัวรับรู้ทางคัลลาริเมทริกและฟลูออเรสเซนต์ มีหมู่ซาลิกซาลเลาดีไฮด์เป็นหน่วยตรวจจับไซยาไนด์ สามารถเตรียมได้โดย 4 ขั้นตอนจากไพโรล ได้ผลิตภัณฑ์ร้อยละ 71 และ 80 ตามลำดับ การใช้ประโยชน์ของอิเล็คโทรฟิลิกของหมู่แอลดีไฮด์ปฏิกิริยาการเติมแบบนิวคลิโอฟิลิกของไซยาไนด์แอนไอออนสามารถเปลี่ยนหมู่แอลดีไฮด์ซึ่งเป็นหมู่รับรู้เป็นไซยาโนไฮดริน และมีผลให้สีค่าดูดกลืนแสงและค่าคายแสงเปลี่ยนไป ในสารละลายDMSO และน้ำ หลังเติมไซยาไนด์ตัวรับรู้ GSB และ RSB มีการเปลี่ยนแปลงจากสีส้มและสีม่วงเป็นไม่มีสี นอกจากนี้ GSB มีการขยายสัญญาณทางฟลูออเรสเซนต์ที่ความยาวคลื่น 504 นาโนเมตร ขณะที่ RSB มีการเปลี่ยนแปลงของค่าการคายแสงจาก 600 เป็น 504 นาโนเมตรหลังจากเติมไซยาไนด์ สำหรับแอนไอออนอื่นๆอีก 13 ชนิดไม่รบกวนการตรวจวัดไซยาไนด์อย่างมีนัยสำคัญ ความเข้มข้นต่ำที่สุดที่ GSB และ RSB สามารถตรวจจับได้อยู่ที่ 0.88 และ 1.79 ไมโครโมลาร์ตามลำดับ ซึ่งมีค่าต่ำกว่าที่องค์การอนามัยโลก หรือ WHO กำหนดไว้สำหรับสารไซยาไนด์ในน้ำดื่มไม่เกิน 2.7 ไมโครโมลาร์ นอกจากนี้การคำนวณด้วยทฤษฎีฟังก์ชันนอลความหนาแน่นสนับสนุนกลไกการเกิดปรากฏการณ์ PET และการขัดขวางในระบบพายน์คอนจูเกตเมื่อเติมไซยาไนด์ลงไประหว่างหมู่ซาลิกซาลเลาดีไฮด์และแกน BODIPY การศึกษาการแสดงภาพเซลล์ แสดงให้เห็นว่า GSB และ RSB เข้ากับเซลล์ได้และสามารถใช้ในการตรวจวัดไซยาไนด์ในเซลล์สิ่งมีชีวิต

สาขาวิชา ปิโตรเคมีและวิทยาศาสตร์พอลิเมอร์ ลายมือชื่อนิสิต .....

ปีการศึกษา 2557 ลายมือชื่อ อ.ที่ปรึกษาหลัก .....

ลายมือชื่อ อ.ที่ปรึกษาร่วม .....

5572250223 : MAJOR PETROCHEMISTRY AND POLYMER SCIENCE
KEYWORDS: BODIPY / CYANIDE / FLUORESCENCE SENSOR / COLORIMETRIC SENSOR

RANGSARIT SUKATO: CONJUGATED BODIPY-SALICYLALDEHYDE PROBES AS FLUORESCENT AND COLORIMETRIC CYANIDE SENSORS. ADVISOR: ASST. PROF. SUMRIT WACHARASINDHU, Ph.D., CO-ADVISOR: PROF. MONGKOL SUKWATTANASINITT, Ph.D., 4 pp.

The development of selective cyanide detection is becoming an increasing demand because it is the one of the most toxic anion that is very harmful to human health and environment. Herein, two new colorimetric and fluorescent probes (GSB and RSB) based on boron dipyrrole-methene (BODIPY) containing salicylaldehyde group for cyanide detection are successfully prepared in 4 steps from the corresponding pyrroles in 70-80 %yield. Taking the advantage of the electrophilic property of aldehyde, nucleophilic addition of cyanide anion can convert salicylaldehyde into cyanohydrin which trigger the color, absorption and emission changes in the probes. In aqueous DMSO/water GSB and RSB undergo exclusive colorimetric changes from orange and purple to colorless upon the addition of cyanide. Moreover, GSB exhibited selective fluorescence turn-on at 504 nm while RSB displayed large blue shift from 600 to 504 nm upon the addition of cyanide. Other 13 anions gave almost no interference under physical condition. The detection limit of cyanide-sensing GSB and RSB are 0.88 and 1.79 μM, respectively which is lower than the concentration limited by World Health Organization (WHO) in drinking water (2.7 μM). A calculation from density functional theory (DFT) supports the cyanide suppress the photoinduced electron transfer (PET) mechanism along with the interruption of π-conjugation between salicylaldehyde and BODIPY core. Cell imaging studies demonstrated that GSB and RSB are compatible and capable of sensing cyanide anion in living cell.

Field of Study:	Petrochemistry and Polymer Science	Student's Signature .....
		Advisor's Signature .....
Academic Year:	2014	Co-Advisor's Signature .....

ACKNOWLEDGEMENTS

I would like to express my deep gratitude to my advisor, Assistant Professor Dr. Sumrit Wacharasindhu, my co-advisor Professor Dr. Mongkol Sukwattanasinitt for their generous advice, invaluable guidance and encouragement throughout the course of this research

I would like to gratefully acknowledge the committee, Assistant Professor Dr. Warinthorn Chavasiri, Assistant Professor Dr. Nuanphun Chantarasiri and Dr. Gamolwan Tumcharern for their comments, guidance and extending cooperation over my presentation. I would like to thank Associate Professor Dr. Paitoon Rachtasakhon, Dr. Anawat Ajavakom and Dr. Sakulsuk Unarunotai for their attention and suggestions during our research group meeting.

I would like to express my gratitude to Material Advancement via Proficient Synthesis group (MAPS), Department of Chemistry, Faculty of Science, Chulalongkorn University for providing the chemicals and facilities throughout the course of study.

A deep affectionate gratitude is acknowledged to my beloved family for their understanding, encouragement and support throughout the education course. I especially thank Narongpol Kaewchangwat, Sattaya Suklim, Nopparat Thavornsin, Kunnikar Vongnam and Pornpat Sam-ang for their suggestions and guidance. I would like to thank all of my friends for their friendship, expecially Watanya Krailat, Suthikorn Jantra, Apiwat Promchat and Jade'tapong Klahan for their help during the course of my graduate research. Moreover, I would like to thank Associate Professor Dr. Tanapat Palaga and Nuanphun Sangpetch for their help and suggestion during the course of cell imaging. I would like to thank all of my friends in over research group for their great friendships and suggestions.

Finally, I would like to express my thankfulness to my beloved parent who always stand by me side during both of my pleasant and hard time.

CONTENTS

Page

Page

LIST OF TABLES

Table Page

LIST OF FIGURES

LIST OF SCHEMES

Scheme Page

LIST OF ABBREVIATIONS

A	acceptor
Ar	aromatic
Calcd	calculated
^{13}C NMR	carbon-13 nuclear magnetic resonance
$CDCl_3$	deuterated chloroform
D	donor
d	doublet (NMR)
dd	doublet of doublet (NMR)
ESIMS	electronspray ionization mass spectrometry
Equiv	equivalent (s)
g	gram (s)
^{1}H NMR	proton nuclear magnetic resonance
Hz	Hertz
HRMS	high resolution mass spectrum
h	hour (s)
ICT	internal charge transfer
J	coupling constant
mg	milligram (s)
mL	milliliter (s)
mmol	millimole (s)
m/z	mass per charge
m	multiplet (NMR)
M.W.	molecular weight
M	molar
MHz	megahertz
rt	room temperature
s	singlet (NMR)
TEA	triethylamine

THF	tetrahydrofuran
UV	ultraviolet
δ	chemical shift
°C	degree Celsius
µL	microliter (s)
µM	micromolar (s)
Φ	quantum yield

CHAPTER I
INTRODUCTION

1.1 Overview

Cyanide ion is very toxic to human or animal even at low concentration can cause death. It can enter to the human or animal body. However, cyanide has been wildly used in chemical industrial, agricultural, X-ray film recovery, mining, jewelry manufacturing [1]. Even in nature, some kind of plant or living organism can produce or release cyanide to the environment [2]. To determine the presence of cyanide ion in water, there are two main methods colorimetric change and the titration technique. Among analytical techniques for the detection of CN^-, fluorescence spectroscopy is one of the most sensitive method for detection cyanide. They use fluorophore attached to receptor probe. Nowadays, there used many types of fluorophore for cyanide detection, for example, phenazine [3], naphthalene [4] or Dipyrrole [5]. In this work, we use boron dipyrromethene (BODIPY) as the fluorophore unit and salicyladehyde as the receptor moiety to create molecular sensor for detection of cyanide.

1.2 Introduction of cyanide (LOD, method)

Cyanide is the one of the most toxic compound. When able to enter into the blood system by ingestion, skin absorption or inhalation and will interact with a heme unit in the cytochrome active site [6]. There are two main methods for determination of cyanide, first is colorimetric which is monitor the color change by the UV-absorption and eye observation. The second is the titration technique using $AgNO_2^-$ as titrant. At the end point, $AgNO_2^-$ will react with CN^- and from the $Ag(CN)_2^-$ complex. This method required time, highly skill technician and has a relatively low sensitivity. According to this concern, the World Health Organization (WHO) set the maximum contaminant value of cyanide in drinking water is 2.7 μM [7].

1.3 Introduction of fluorescence

Fluorescence activity can be schematically illustrated with the classical Jablonski diagram (**Figure 1.1**) to describe absorption and emission of light [8, 9]. Prior to excitation, the electronic configuration of the molecule is described as being in the ground state (**S0**). When a fluorophore absorbs light energy, it is usually excited to a higher vibrational energy level in the first excited state (**S1**) before rapidly relaxing to the lowest energy level when transition from the upper to lower bars in (**S1**), is termed vibrational relaxation or internal conversion and occurs in about a picosecond or less. Fluorescence lifetimes are typically four orders of magnitude slower than vibrational relaxation, giving the molecules sufficient time to achieve a thermally equilibrated lowest-energy excited state prior to fluorescence emission.

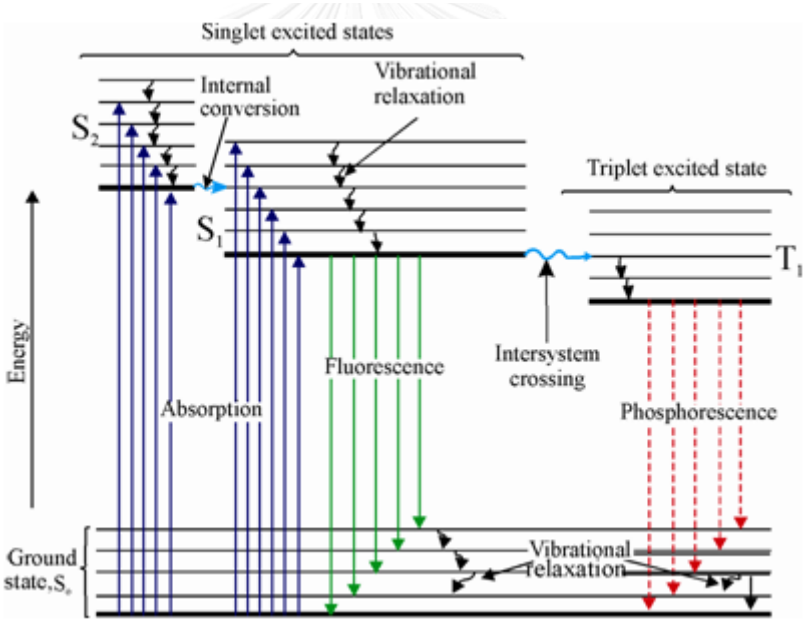

Figure 1.1 Jablonski energy diagram explaining fluorescence processes.

1.3.1 Structure of fluorescence compounds (mode on-off)

Nowadays, chemical and biological sensing system has been used due to it had rapid detection result and high selectivity. All methods have been developed and improved using redox [10], chromogenic [11] or flurogenic [12] changes as the detection signals. Conjugated polymers (CPs) have emerged as one of the most important classes

of transducing materials. They transform a chemical signal to easily measurable electrical or optical events. Fluorescence based methodologies have attracted much interest due to their intrinsic sensitivity and selectivity [13]. Considerable efforts have been devoted to the design of fluorescent compounds to be used as transducers. CPs with delocalized **π**-electron system have an overpowering interest due to their versatile optical and electrical properties [14]. **Figure 1.2** shows structures of variety of CPs commonly investigated, including polythioprene (1) [15], polypyrrole (2) [16], polyfluorene (3) [17], poly(para-phenylenevinylene) (4) [18] and poly(para-phenyleneethynylene) (5) [19]. The delocalized electronic structure of CPs enables them to exhibit efficient absorption, strong emission and produce amplified signal change upon interacting with various analytes.

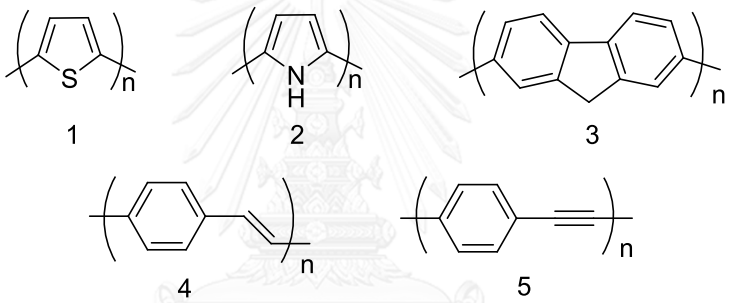

Figure 1.2 Molecular structure of some common conjugated polymers (CPs)

1.3.2 Mechanisms

- Internal charge transfer (ICT)

In some case, molecule in the locally excited (LE) state may undergo to the other pathway and release the energy without emission or non-radiative decay. Example, a substance with structure composed of both good electron donating and withdrawing groups by electron delocalization process can delocalize electron pair within the molecule which is called internal charge transfer (ICT) process to convert to the ICT excited state (**Figure 1.3**). This state has lower energy with different geometry from the LE state. After ICT excited state relax to the original ground state.

This relaxation may give light either within or outside the visible light spectrum [20-28]. Accord to multi-step processes, ICT emission usually has lower fluorescence quantum yield comparing with the LE state. The ICT state usually gives longer wavelength and is usually stabilized by polar solvent due to ICT excited state stabilization [29, 30].

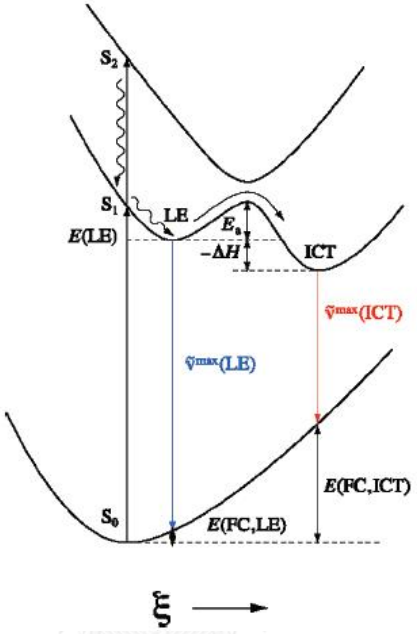

Figure 1.3 The potential energy surface of the ground state (S_0) is excited to S_1 or S_2 then relaxed to the LE state and ICT state (FC = Franck Condon).

- Photoinduced electron transfer (PET)

When the fluorophore is excited, the electron in the highest occupied molecular orbital (HOMO) is promoted to the lowest unoccupied molecular orbital (LUMO). This enables the electron transfer from the HOMO of the donor (belonging of the free cation receptor) to that of the fluorophore (**Figure 1.4, A**) resulting in low or undetectable emission. When this system is in present of the analyte, the energy of bound receptor will be lower, thus the PET can be disrupted and the system can emit fluorescence upon excitation (**Figure1.4, B**).

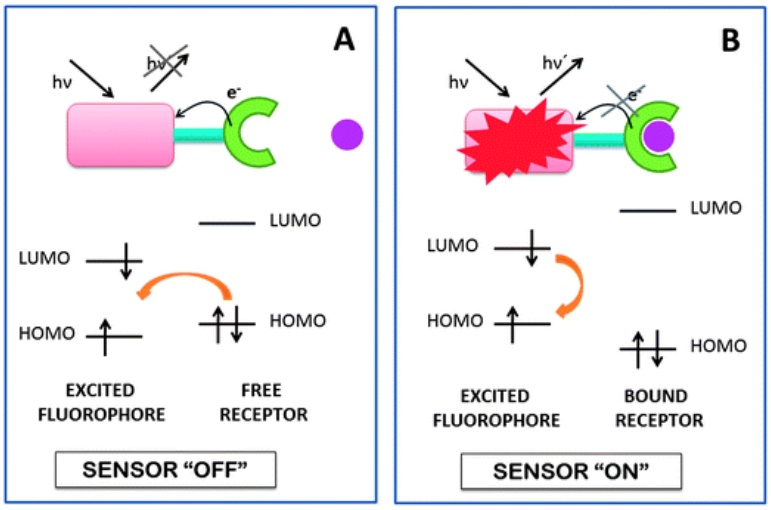

Figure 1.4 Principle of the PET mechanism.

1.4 Literature review on fluorescence sensors for cyanide ion

Due to nucleophilic properties of cyanide ion, most of cyanide sensors were designed to incorporate electron deficient groups to enable the addition reaction of cyanide ions.

2013, Yang et al. [3] reported **Probe 2** containing dicyano vinyl group as a blinding unit and use phenazine as the fluorophore (**Figure 1.5**). At the initial state, it had ICT process and emited red fluorescence at 720 nm which had low quantum yield. After addition of cyanide, the ICT process was destroyed and **Probe 2** brought the strong orange emission at 630 nm showing a detection limit ca. 5.77×10^{-2} μM.

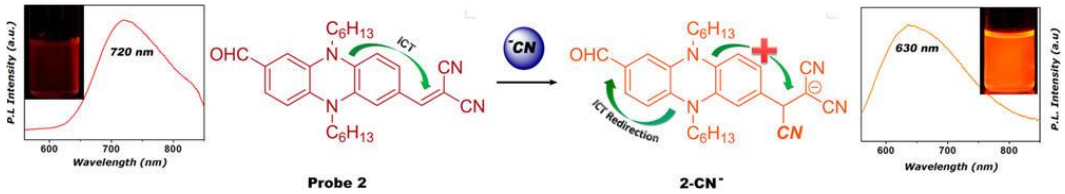

Figure 1.5 The mechanism of cyanide ion monitoring of phenazine derivatives (**Probe 2**).

In 2014, Li et al. [31] synthesized fluorescent chemosensor (**S1**) based on benzimidazole group for cyanide anion in aqueous solution (H_2O/DMSO, 8:2, v/v) (**Figure 1.6**). The fluorescence color of the solution containing sensor **S1** induced a

remarkable color change from pale blue to mazarine only after the addition of CN^- in aqueous solution. Moreover, the detection limit on fluorescence response of the sensor to CN^- is down to 8.8 x 10^{-8} M.

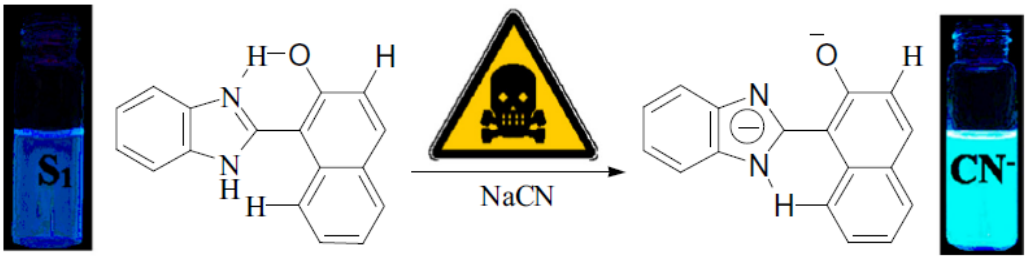

Figure 1.6 The mechanism of receptor **S1** for cyanide ion.

Recently, in 2014, Niamnont et al., [32] discovered that salicylaldehyde derivatives can be used as a selective probe for cyanide ion in HEPES buffer media with 1.6 μM of LOD (**Figure 1.7**). The fluorophore exhibited fluorescence turn-on in response to cyanide in aqueous media. The turn-on signal is result of the conversion of the aldehyde to cyanohydrin via the internal acid catalyzed.

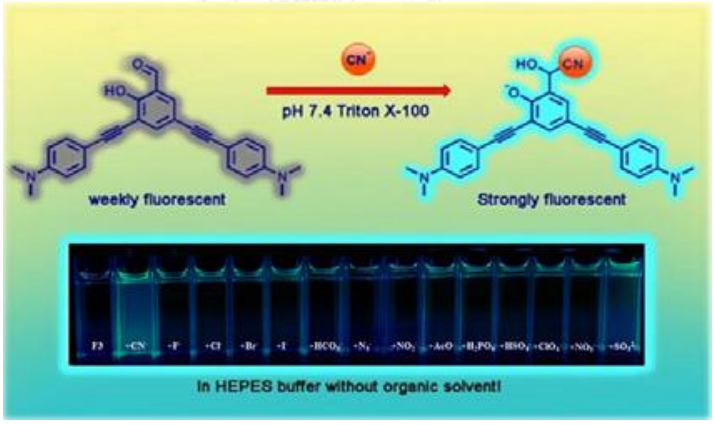

Figure 1.7 Cyanide detection by probe based on cyanohydrin formation.

1.5 Literature review on Boron dipyrromethene (BODIPY)

1.5.1 Introduction of BODIPY

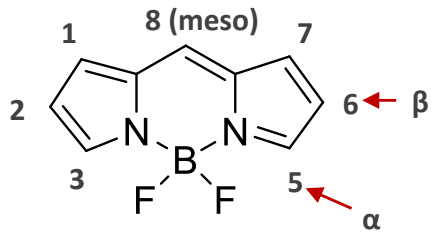

Figure 1.8 The structure and numbering of the BODIPY fluorophore

Boron dipyrromethene or BODIPY was first discovered in 1968 by Treibs and Kreuzer [33] and has been used as the optical materials for many applications such as organic dyes [34] and small-molecule solar cells [35]. The core structure of the BODIPY fluorophore is shown in **Figure 1.8.** BODIPY contains a boron atom as part of the core structure. The advantages of BODIPY are stable in physiological conditions, relatively insensitive to variations in pH, generally have high quantum efficiency, sharp emission peaks, tunable in fluorescence characteristic and compatible with biological media. Which these advantages, in the past few years, there have many reports the fluorescence for the detection of toxic chemical such as metal ions. However, there was only few reports on anion based on BODIPY derivatives in water and even in living cell.

1.5.2 Literature review on BODIPY-based fluorescence sensors toward cyanide ion

In 2008, Ekmekci et al. [34] developed and synthesized the flurogenic and colorimetric probe based on BODIPY for the cyanide ion detection (**Figure 1.9**). Trifluoro amide receptor attached on the 3-position of BODIPY core demonstrated fluorescence quenching along with color change from pink to blue after the addition of cyanide anion.

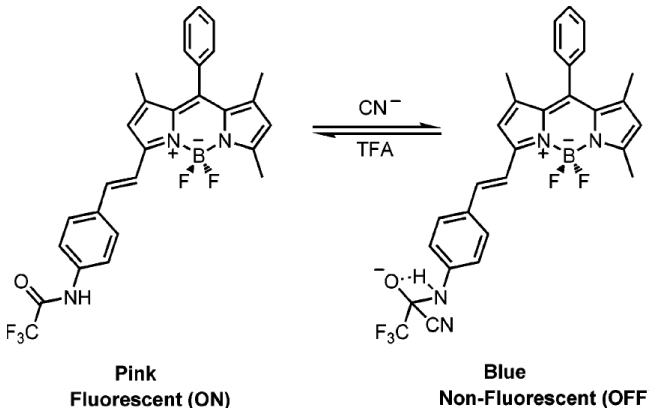

Figure 1.9 Suggested mechanism for on-off switching within the presence of CN- ions

In 2012, Madhu et al. [35] successfully synthesized the BODIPY fluorophore containing aldehyde receptor moiety at the 8 position (**Figure 1.10**). When cyanide ion reacted with the carbonyl group by nucleophilic addition reaction with the carbonyl group, it was converted into the corresponding cyanohydrin. Upon addition of cyanide, this probe gave an apparent color change from orange to dark yellow and turn off fluorescence with 3 ppm of detection limit. Moreover, this BODIPY probe can also be used in biological cell lines for the detection of cyanide ion.

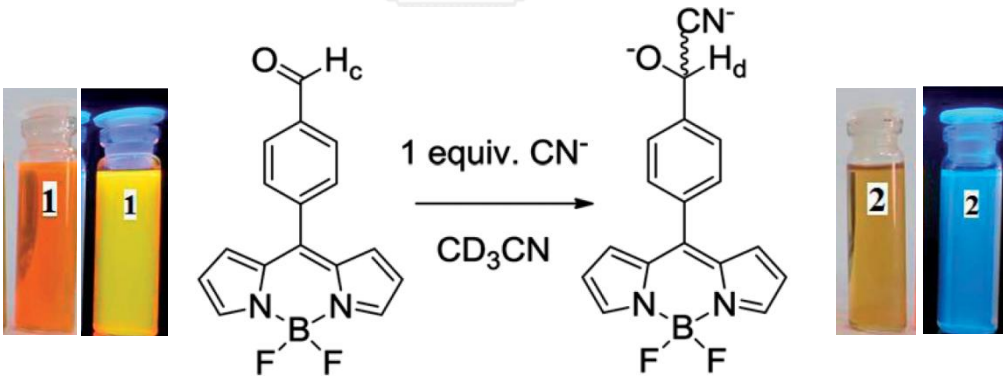

Figure 1.10 The nucleophilic addition reaction of cyanide toward probe and colorimetric and flurogenic change before and after addition of cyanide.

In 2012, Zhang et al. [36] reported the BODIPY containing indolium iodide (**4b**) (**Figure 1.11**). In the present of cyanide **3b** showed the ratiometric fluorescence response to cyanide anion with a dramatic fluorescence color change from red to green showing a detection limit ca. 0.5 μM. However, this system had to perform at basic condition (pH 9.3)

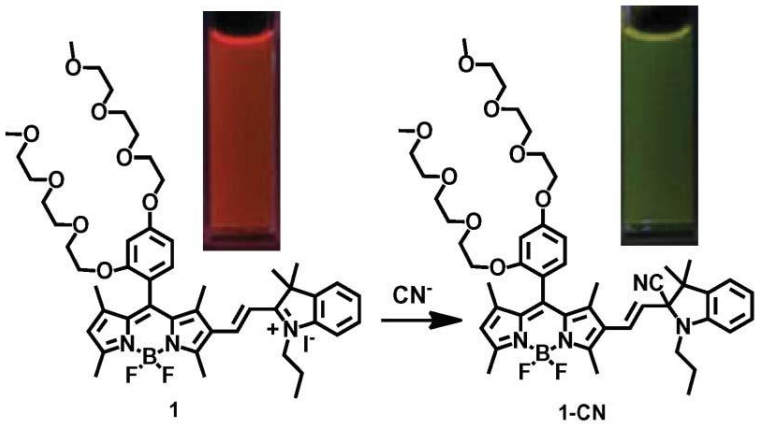

Figure 1.11 Ratiometric fluorescent response of probe **1** to cyanide ions, with a dramatic fluorescence color change from red to green.

In 2012, Lee et al. [37] successfully synthesized BODIPY **1** containing dicyano-vinyl group as turn-on fluorescence sensor for cyanide anion in 1%THF/H_2O. The photoinduced intramolecular charge transfer (ICT) from the BODIPY unit to the dicyano-vinyl group could occur resulting from the nucleophilic attack of cyanide on the olefinic carbon. This caused the interruption of **π**-conjugation between the phenyl and dicyano-vinyl groups, which would influence the fluorescence emission.

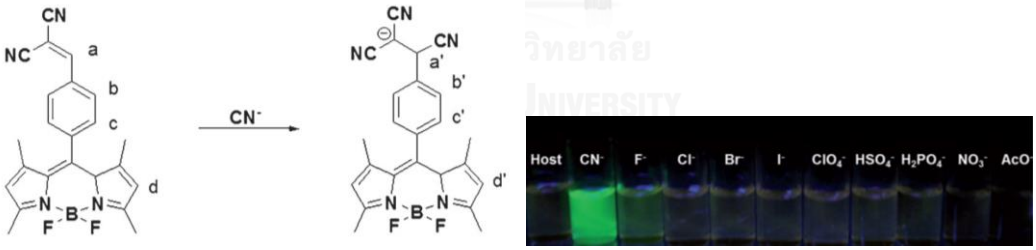

Figure 1.12 Structure of **1** and its CN^- adduct (left) and **1** solutions with various anions under black light (right).

Based on above literature reviews on BODIPY for cyanide sensors, there are some disadvantages such as lack of colorimetric change, turn-off fluorescence and ability to perform in physical condition (pH 7.4). Therefore, colorimetric, turn-on fluorescence chemosensor for cyanide detection with high sensitivity and biological compatibility are very limited.

1.6 Objective and expected outcome of this work and expected outcome

In this research, we design and prepare two fluorescence chemosensors based on BODIPY derivatives (**GSB** and **RSB)** containing salicylaldehyde moiety as the receptor unit. We expect turn-on fluorescence mode for cyanide detection along with naked eye observation, high selectivity and sensitivity toward cyanide ion in aqueous media. Moreover, we will use our BODIPY in biological media in order to detect cyanide in cells sample.

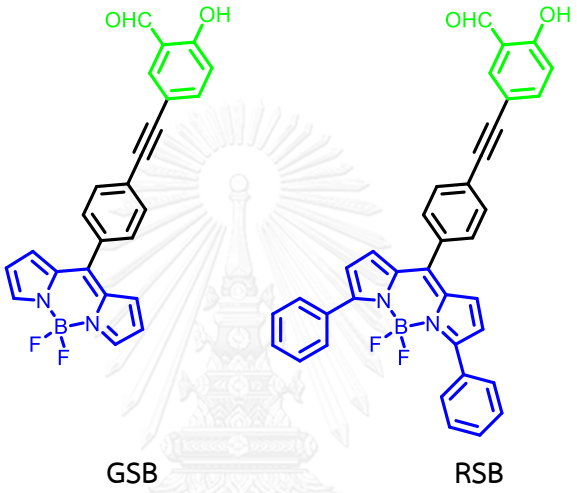

GSB **RSB**

Figure 1.13 The structures of target molecules.

CHAPTER II

EXPERIMENT

2.1 Chemical and Materials

Bis(triphenylphosphine)palladium(II) dichloride ($PdCl_2(PPh_3)_2$), trimethylsilyl-acetylene and triphenylphosphine were purchased from Fluka. Copper (I) iodide and 2-hydroxybenzaldehyde were purchased from Aldrich. 4-Iodobenzaldehyde was purchased from TCI. Calcium carbide and all other reagents were non-selectively purchased from Sigma-Aldrich, Fluka or Merck and used without further purification. For most reactions, solvents such as dichloromethane is reagent grade stored over molecular sieves. In anhydrous reactions, solvents such as THF and TEA were dried and distilled before use according to the standard procedures. All column chromatography was operated using Merck silica gel 60 (70-230 mesh). Thin layer chromatography (TLC) was performed on silica gel plates (Merck F245). Solvents used for extraction and chromatography such as dichloromethane, hexane and ethyl acetate were commercial grade and distilled before use while diethyl ether was reagent grade. Mili-Q water was used in all experiments unless specified otherwise. All of reactions were carried out under positive pressure of N_2 filled in rubber balloons.

2.2 Analytical Instruments

The ^1H and ^{13}C-NMR spectra were acquired from sample solution in $CDCl_3$, D_2O and DMSO-d_6 on a Varian Mercury NMR spectrometer, which operated at 400 MHz for ^1H-NMR and 100 MHz for ^{13}C-NMR. Mass spectra were obtained by electrospray ionization mass spectrometry (ESI). Absorption spectra were measured by a Varian Cary 50 UV-Vis spectrophotometer (Varian, USA) and emission spectra were obtained from a Varian Cary Eclipse spectrofluorometer (Varian, USA).

2.3 Synthesis of GSB and RSB

2.3.1 Preparation of 2-hydroxy-5-iodobenzaldehyde (2)

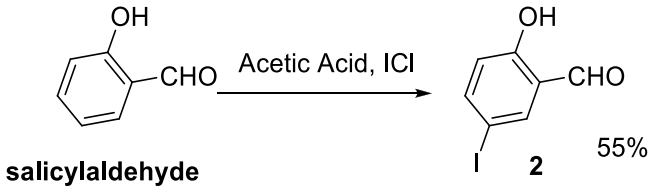

Scheme 2.1 Synthesis of **2**

To a prepared mixture of salicylaldehyde (5.0 g, 0.041 mol), iodo-monochloride (8.12 g, 0.05 mol) and acetic acid (3.0 g, 0.05 mol) were stirred in round bottle flask at ambient condition for 18 h. The reaction mixture was extracted with CH_2Cl_2 for three times. The combined extract was washed with DI water, $Na_2S_2O_3$ and $NaHCO_3$ then dried over anhydrous $MgSO_4$ and purified by column chromatography on silica gel to afford the pure product of 2.717 g (27%) as white solid. ^{1}H NMR (400 MHz, $CDCl_3$) δ 10.93 (d, *J* = 1.0 Hz, 1H), 9.81 (d, *J* = 0.7 Hz, 1H), 7.83 (d, *J* = 2.0 Hz, 1H), 7.74 (d, *J* = 8.8 Hz, 1H), 6.78 (d, *J* = 8.8 Hz, 1H).

2.3.2 Preparation of 2-Hydroxy-5-((trimethylsilyl)ethynyl)benzaldehyde (3)

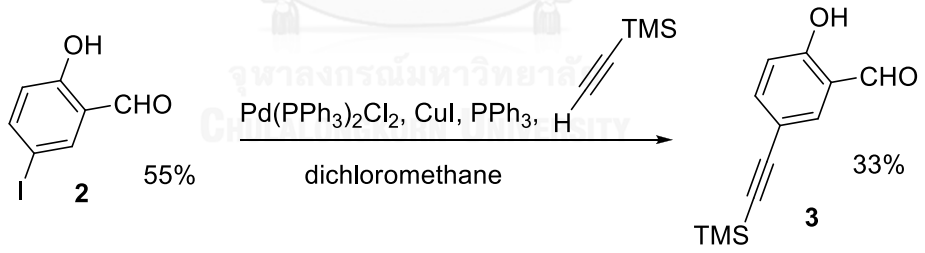

Scheme 2.2 Synthesis of **3**

2-Hydroxy-5-iodobenzaldehyde (1.0 g, 4.03 mmol), bis(triphenylphosphine)-palladium(II) dichloride (85 mg, 0.121 mmol), CuI (23.04 mg, 0.121 mmol), PPh_3 (21.35 mg, 0.081 mmol) and trimethylsilylacetylene (593.505 mg, 6.05 mmol) were dissolved in a mixed solvent of TEA (5 mL) and THF (30 mL) in round bottle flask with magnetic stir bar. The reaction mixture was stirred at ambient condition for 18 h. After removal of solvent under reduced pressure, the residue was purified by column chromatography on silica gel to give product in 864.000 mg as white solid (98%). ^{1}H

NMR (400 MHz, $CDCl_3$) δ 11.08 (s, 1H), 9.83 (s, 1H), 7.69 (s, 1H), 7.58 (d, *J* = 7.3 Hz, 1H), 6.92 (d, *J* = 8.6 Hz, 1H), 0.23 (s, 11H).

2.3.3 Preparation of 5-ethynyl-2-hydroxybenzaldehyde (4)

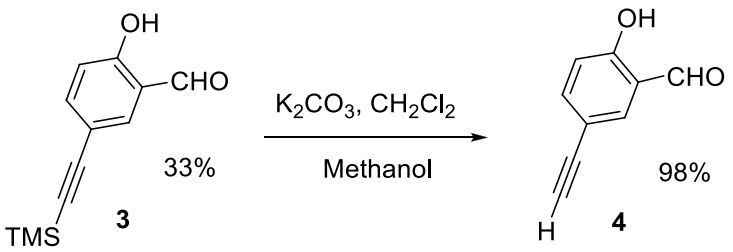

Scheme 2.3 Synthesis of **4**

2-Hydroxy-5-((trimethylsilyl)ethynyl)benza-ldehyde (853 mg, 2.91 mmol) and K_2CO_3 (1403.80 mg, 17.46 mmol) were dissolved in a mixed solvent of CH_2Cl_2 (30 mL) and MeOH (15 mL) in round bottle flask with magnetic bar. The reaction mixture was stirred at ambient condition for 18 h. The reaction was washed with DI water, then dried over anhydrous $MgSO_4$ and purified by column chromatography on silica gel to give desired product in 308 mg as white solid (54%). ^{1}H NMR (400 MHz, $CDCl_3$) δ 11.12 (s, 1H), 9.85 (s, 1H), 7.71 (d, *J* = 2.0 Hz, 1H), 7.61 (dd, *J* = 9.1, 1.7 Hz, 1H), 6.94 (d, *J* = 8.4 Hz, 1H), 3.02 (s, 2H).

2.3.4 Preparation of 2-phenylpyrrole (6b)

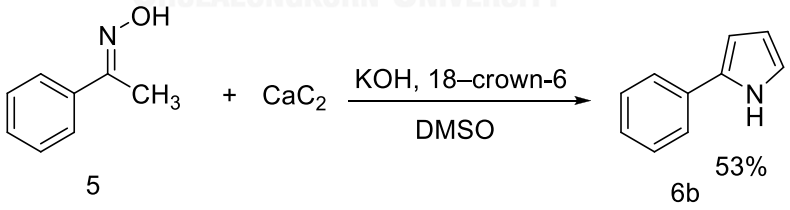

Scheme 2.4 Synthesis of **6b**

Acetophenone oxime (400 mg, 2.96 mmol), calcium carbide (1139 mg, 17.77 mmol), and a piece of 18-crown-6 were dissolved in solvent of DMSO (40 mL) in seal tube with magnetic bar. The reaction mixture was stirred at 100°C for 18 hr, then the reaction mixture was extracted with diethyl ether, washed with DI water and purified by column chromatography on aluminum oxide to give desired product in 224 mg as

dark purple solid (53%). ^{1}H NMR (400 MHz, $CDCl_3$) δ 7.46 (d, *J* = 7.6 Hz, 1H), 7.35 (t, *J* = 7.7 Hz, 1H), 7.19 (t, *J* = 7.4 Hz, 1H), 6.85 (s, 1H), 6.51 (s, 1H), 6.29 (d, *J* = 3.0 Hz, 1H).

2.3.5 Preparation of BODIPY 7a

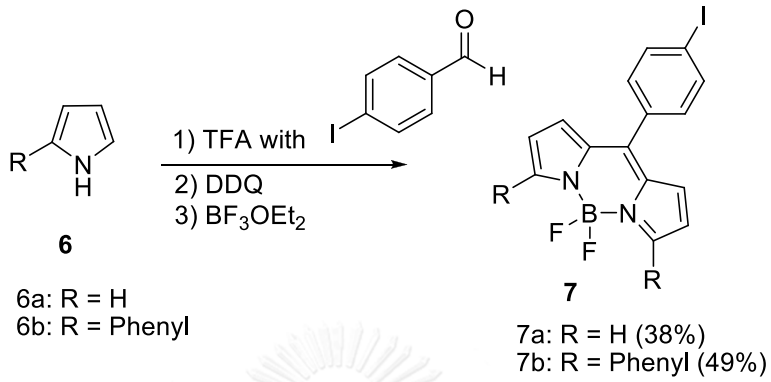

Scheme 2.5 Synthesis of **7a** and **7b**

4-Iodobenzaldehyde (1000 mg, 4.31 mmol), pyrrole (compound **6a**) (578.3 mg, 8.62 mmol) were dissolved in dried CH_2Cl_2 (40 mL) in round bottle flask with magnetic bar. The reaction mixture was stirred at ambient condition for 10 min, trifluoroacetic acid (TFA) was added for 2-3 drops, and the solution was stirred for another 10 min. The solvent was removed under reduced pressure, dissolved in CH_2Cl_2, washed with DI water, dried over anhydrous $MgSO_4$ and removed solvent under reduced pressure then purified by column chromatography on silica gel to give intermediate crude product. The intermediate product (395 mg, 1.135 mmol) and 2, 3-dichloro-5, 6-dicyanobenzoquinone, DDQ (258 mg, 1.135 mmol) was dissolved in dichlorometane (30 ml) in round bottle flask with magnetic stir bar. The reaction mixture was stirred at room temperature for 30 minutes, then the reaction mixture was stirred at 0 degree Celsius. N, N-Diisopropylethylamine (1032.8 mg, 8 mmol) and Boron trifluoride diethyl etherate (1620.84 mg, 11.42 mmol) were added and stirred for another 30 minutes. The reaction was washed with saturated $NaHCO_3$, brine, dried over anhydrous $MgSO_4$ and removed solvent under reduced pressure the purified by column chromatography on silica gel to give product in 570 mg as orange solid (38%). ^{1}H NMR (400 MHz, $CDCl_3$) δ 7.93 (s, 1H), 7.87 (d, *J* = 8.3 Hz, 1H), 7.28 (d, *J* = 8.3 Hz, 1H), 6.89 (d, *J* = 3.4 Hz, 1H), 6.54 (d, *J* = 2.3 Hz, 1H).

2.3.6 Preparation of BODIPY 7b

This compound was prepared from 2-Phenylpyrrole (compound **6b**) using the same procedure for **6a**. The product was obtained as a red solid in 528 mg (49%). ^{1}H NMR (400 MHz, $CDCl_3$) δ 7.93 – 7.79 (m, 1H), 7.47 – 7.35 (m, 1H), 7.31 (d, *J* = 8.3 Hz, 1H), 6.85 (d, *J* = 3.9 Hz, 1H), 6.62 (d, *J* = 3.8 Hz, 1H).

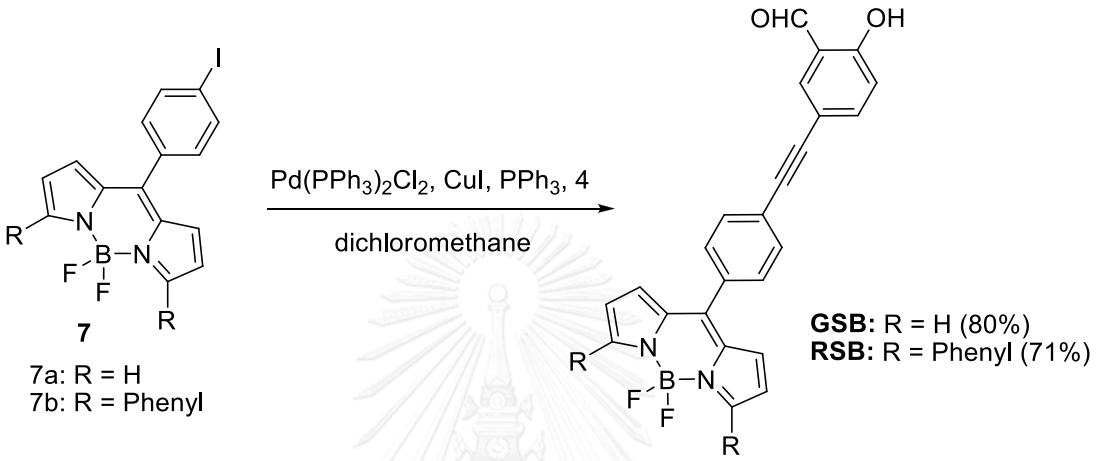

Scheme 2.6 Synthesis of **GSB** and **RSB**

2.3.7 Preparation of GSB

A mixture of compound **7a** (54 mg, 0.1369 mmol), 5-ethynyl-2-hydroxybenzaldehyde **(4)** (40 mg, 0.274 mmol), bis(triphenylphosphine)palladium(II) dichloride (14.04 mg, 0.02 mmol), CuI (3.81 mg, 0.02 mmol) and PPh_3 (2.9 mg, 0.011 mmol) were dissolved in mixture solvent of TEA (3 mL) and THF (15 mL) in round bottle flask with magnetic stir bar. The reaction mixture was stirred at ambient condition for 18 hr. The solvent was removed under reduced pressure, dissolved in CH_2Cl_2 (30 mL), washed with NH_4Cl, DI water, dried with MgSO4 and removed solvent under reduced pressure then purified by column chromatography on silica gel to give desire product in 45 mg as dark green solid (80%). ^{1}H NMR (400 MHz, $CDCl_3$) δ 11.17 (s, 1H), 9.91 (s, 1H), 7.94 (s, 2H), 7.80 (s, 2H), 7.74 – 7.51 (m, 7H), 7.01 (d, *J* = 8.3 Hz, 1H), 6.93 (s, 2H), 6.55 (s, 2H).

2.3.8 Preparation of RSB

This compound was prepared from compound **7b** using the same procedure for **GSB**. The product was obtained as a maroon solid in 148 mg (71%). ^{1}H NMR (400 MHz, $CDCl_3$) δ 11.17 (s, 1H), 9.92 (s, 1H), 7.85 (d, *J* = 5.5 Hz, 4H), 7.81 (s, 2H), 7.71 (d, *J* = 8.5 Hz, 1H), 7.66 (d, *J* = 7.9 Hz, 2H), 7.59 (d, *J* = 8.0 Hz, 3H), 7.41 (d, *J* = 5.4 Hz, 6H), 7.02 (d, *J* = 8.6 Hz, 1H), 6.89 (d, *J* = 3.9 Hz, 2H), 6.63 (d, *J* = 3.7 Hz, 2H).

2.4 Photophysical properties

The stock solutions of 1 mM GSB and RSB in DMSO were prepared and diluted to 100 μM.

2.4.1 UV-Visible spectroscopy

The UV-Visible absorption spectra of the stock solution of fluorophore were recorded from 250 nm to 60 nm at ambient temperature.

2.4.2 Fluorescence spectroscopy

The stock solutions of GSB and RSB were diluted to 10 μM in 90% DMSO and 10% HEPES buffer pH 7.4. The emission spectra of fluorophore were recorded from 350 nm to 700 nm at ambient temperature using an excitation wavelength at 345, 504 and 557 nm, respectively.

2.4.3 Fluorescence quantum yield

The fluorescence quantum yield of fluorophores were perform in DMSO by using quinine sulfate (ΦF = 0.546 in 0.5 N H_2SO_4) and rhodamine B (ΦF = 0.70 in MeOH) as the standard references. The UV-Visible absorption spectra of five analytical samples and five reference samples at varied concentrations were recorded. The maximum absorbance of all solution samples should never exceed 0.1. The fluorescence emission spectra of the same solution using appropriate excitation wavelengths selected were recorded based on the absorption maximum wavelength (λ_{max}) of each compound. Graphs of integrated fluorescence intensity were plotted against the absorbance at the respective excitation wavelengths. Each plot should be straight line

with 1 interception and gradient *m*. In addition, the fluorescence intensity vs. absorbance represented into the following equation.

$$\Phi_X = \Phi_{ST}\left(\frac{Grad_X}{Grad_{ST}}\right)\left(\frac{\eta_X^2}{\eta_{ST}^2}\right)$$

The subscripts Φ_{ST} denote the fluorescence quantum yield of standard reference which used quinine sulfate (Φ = 0.546 in 0.5 N H_2SO_4) and rhodamine B (Φ = 0.70 in MeOH) and Φ_X is the fluorescence quantum yield of sample and η is the refractive index of the solvent.

2.5 Fluorescence sensor study

2.5.1 Anion sensor

The excitation wavelength was 345 nm, 504 nm and 557 nm for GSB and RSB and the emission was recorded from 355-750 nm. Sodium anion solutions were prepared in Milli-Q water. Concentrations of all stock sodium anion solution were adjusted to 50 mM and were added with desired volumes (10 µL) to the fluorophore solutions. The final volumes of the mixture were adjusted to 1000 µL to afford the final concentration of 10 µM for the fluorophore and 700 µM for anions.

2.5.2 Surfactant study

The excitation wavelength were 504 nm and 557 nm and the emission was recorded from 514-750 nm. Surfactant solutions were prepared in Milli-Q water. Concentration of all stock sodium anion solutions were adjusted to 20 mM and were added with the desired volume (700 µL) to fluorophore solutions. The final volumes of the mixture were adjusted to 1000 µL to afford the final concentration of 10 µM for the fluorophores and 10 µM for surfactants.

CHAPTER III

RESULTS AND DISCUSSION

3.1 Cyanide fluorescence sensor from GSB and RSB

In this work, we designed and synthesized the fluorophores **GSB** and **RSB** based on the salicylaldehyde probe attached to BODIPY fluorogenic unit with unsubstitution and extended phenyl group at 3, 5 position. It should make these fluorophore for turn-on and colorimetric fluorescence sensor for CN^- detection and can be used in cell imaging application under physical condition.

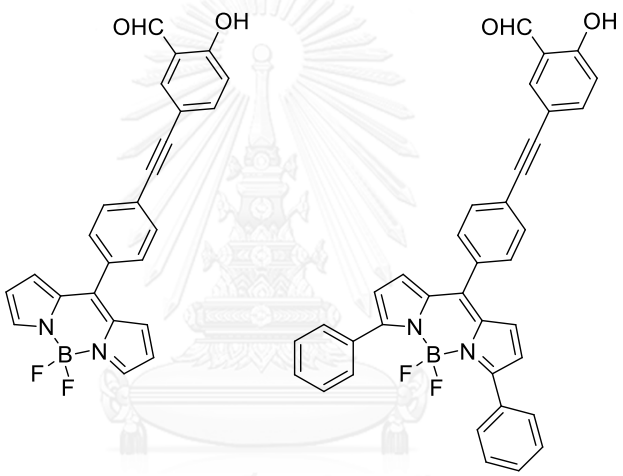

GSB **RSB**

Figure 3.1 Fluorophore molecules **GSB** and **RSB.**

3.1.1 Synthesis and characterization of GSB and RSB

The fluorophore **GSB** and **RSB** were synthesized as shown in **Scheme 3.1**. The synthesis was started with the iodination of salicylaldehyde with iodine monochloride using acetic acid to give **2** in 55% yield. Then Sonogashira coupling reaction between 2-hydroxy-5-iodobenzaldehyde and trimethylsilylacetylene followed by desilylation afforded 5-ethynyl-2-hydroxybenzaldehyde (**4**) in excellent yield. For the BODIPY core synthesis (**8a** or **8b**), it was accomplished with the known reaction sequence: condensation of unsubstituted pyrrole or 2-phenylpyrrole with 4-iodobenzaldehyde, oxidation with 2,3-Dichloro-5,6-dicyano-1,4-benzoquinone (DDQ) and complexation with Boron trifluoride diethyl etherate. Finally, the Sonogashira coupling reaction

between BODIPY fluorophores (**8a** or **8b**) and 5-ethynyl-2-hydroxybenzaldehyde gave **GSB** and **RSB** in 80 and 71% yield, respectively.

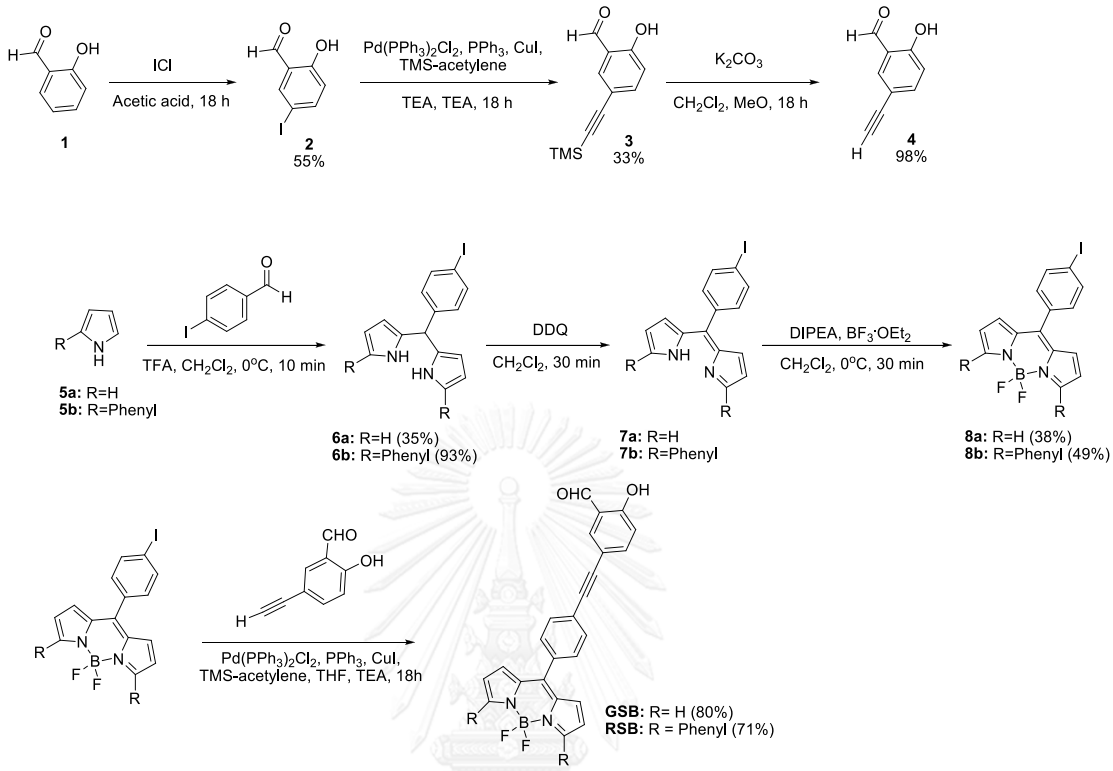

Scheme 3.1 Synthesis route of fluorophore **GSB** and **RSB**.

For the NMR characterization, ^{1}H NMR spectrum of 5-ethynyl-2-hydroxybenz-aldehyde (**4**) are shown in **Figure 3.2**. Aldehyde (f), hydroxyl (e), terminal alkyne (b) and aromatic protons (a) showed the corresponding singlet peaks at 11.14, 9.87 and 7.72 ppm, respectively. In addition, the remaining aromatic protons (d and e) displayed at 7.63 and 6.96 ppm, respectively.

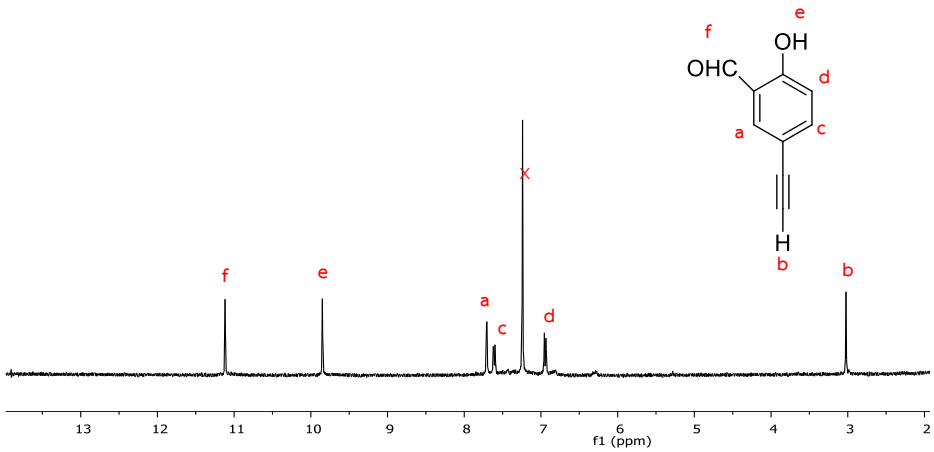

Figure 3.2 ^{1}H NMR spectrum of 5-ethynyl-2-hydroxybenzaldehyde (**4**).

The ^{1}H NMR spectrum of **GSB** and **RSB** are shown in **Figure 3.3**. The present of salicylaldehyde receptors in BODIPY **GSB** and **RSB** were confirmed by the OH (h) peak and carbonyl (i) peak at ca. 9.87 and 11.12 ppm. Both **GSB** and **RSB** showed the characteristic pyrrole peaks (c and d) at ca. 6.84 and 6.59 ppm suggesting the existing of BODIPY core. Moreover, the extra phenyl conjugate of RSB peaks (k, l) showed the signals at ca. 7.39 and 7.37 ppm. Moreover, the molecular weights of **GSB** and **RSB** were confirmed by mass spectrometer (412.119 and 564.821) as seen in appendix (figure S.11 and S.14).

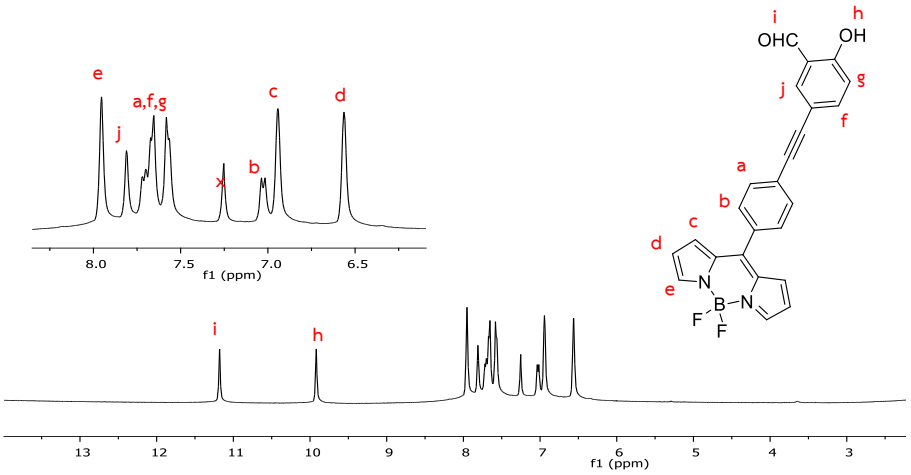

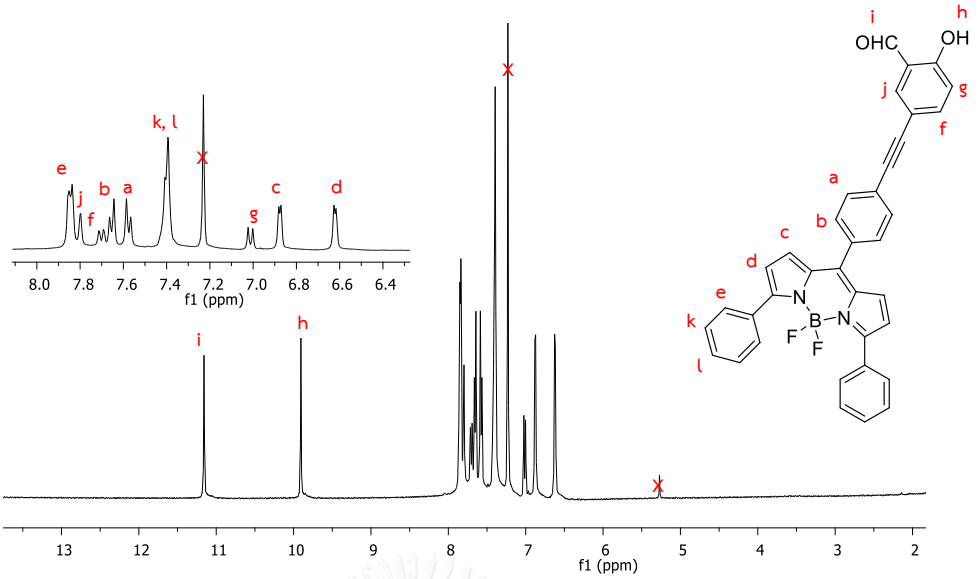

Figure 3.3 ^{1}H NMR spectra of **GSB** and **RSB.**

3.1.2 Photophysical properties of GSB and RSB

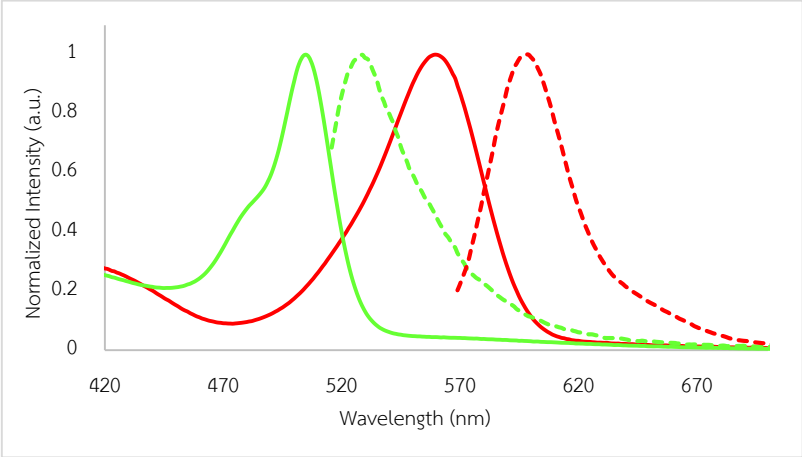

Figure 3.4 Electronic absorption and emission spectra of **GSB** (green) and **RSB** (red) (10μM) in 90%DMSO/TRIS buffer pH 7.4.

The absorption and emission of GSB and RSB were studied in the mixture of DMSO and TRIS pH 7.4 (9:1) solvent. The photophysical properties are compiled in Table 3.1. GSB and RSB fluorophores exhibited absorption maxima at 504 and 557nm, respectively (Figure 3.4). Each fluorophore showed a single maximum emission wavelength at 529 and 600 nm. This resulted in the green and red emission of GSB and RSB under the blacklight. The quantum efficiency of both fluorophores were determined using quinine sulfate (ΦF = 0.546 in 0.5 N H2SO4) and rhodamine B (ΦF

= 0.70 in MeOH) as standard. As expected, GSB and RSB provided relatively low quantum yield than typical BODIPY derivative. The molar absorptivity of both fluorophore were measured (Figure 3.5). GSB and RSB provided the molar absorptivity around 44000 – 45000. The values are corresponded to typical BODIPY derivatives.

Table 3.1 Photophysical properties of **GSB** and **RSB** in 90% DMSO/TRIS buffer pH 7.4.

Compound	Solution	Blacklight	λ_{ab} (nm)	λ_{em} (nm)	Epsilon	Φ_F (%)
GSB			504	529	44000	1
RSB			557	600	45200	13

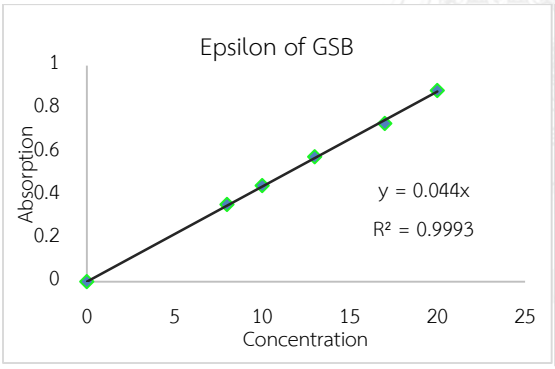

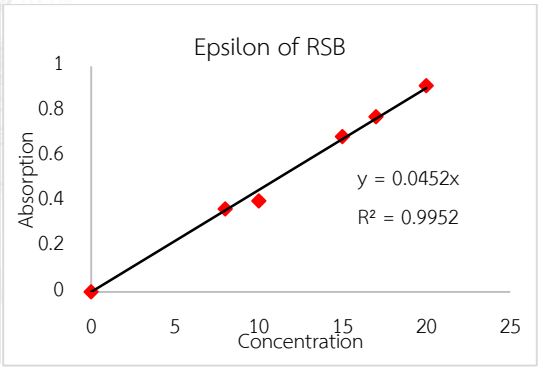

Figure 3.5 The epsilon value of **GSB** (left) and **RSB** (right).

The low quantum yield of **GSB** and **RSB** could be expended by PET and ICT processes as depicted in **Figure 3.6**. For ICT process, the aldehyde moiety will act as electron withdrawing group while hydroxyl moiety will act as electron donor group causing the fluorescent quenching. Also the PET process are occur from the electron transfer between hydroxy donor group and BODIPY acceptor. Moreover, the higher quantum yield of RSB than GSB is probably governed by the photoinduced the electron transfer process (PET) of extra phenyl groups to acceptor BODIPY core which lower the effect of PET from the hydroxy group in salicylaldehyde.

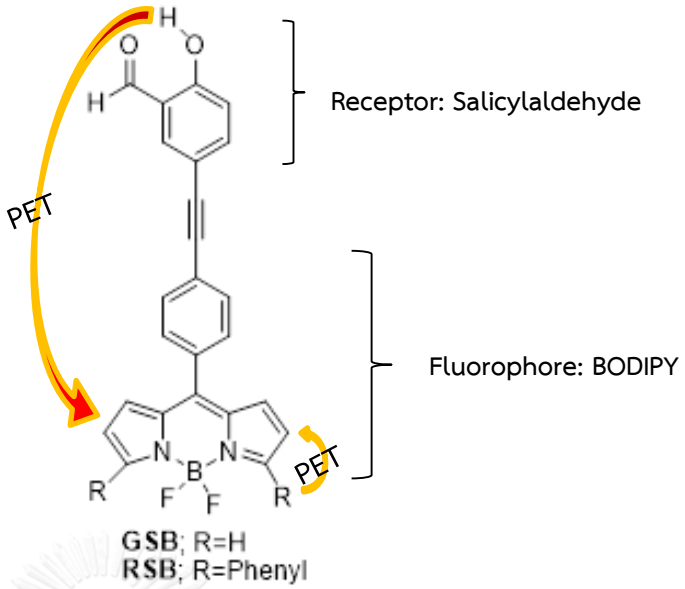

Figure 3.6 Quenching mechanism of photosphere **GSB** and **RSB**

The effects of solvent on emission of fluorophores were studied by varying the content of the TRIS buffer pH 7.4 in the DMSO solution from 10 to 90%, as seen in **Figure 3.7**. The results showed that in high water content, both fluorophores exhibited weak emission due to their poor solubility. Therefore, we decided to use 90% DMSO as the optimum condition for further study.

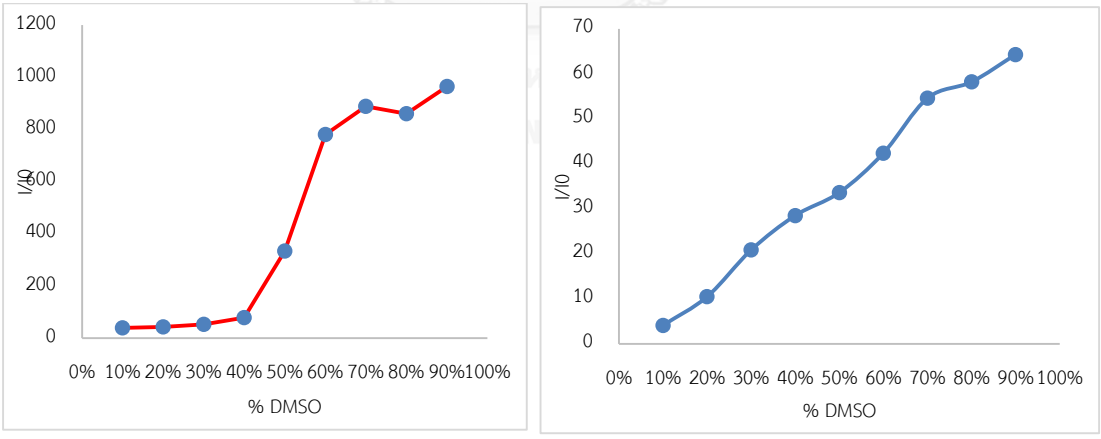

Figure 3.7 Fluorescence enhancement ratio (I/I_0) of **GSB** (left) and **RSB** (right) (10μM) in TRIS buffer pH 7.4 mixed with DMSO (10-90% v/v).

3.1.3 Optical response of GSB and RSB toward cyanide and other anions

To evaluate **GSB** and **RSB** as the cyanide sensors, the absorption spectrum of each fluorophore before and after the addition of cyanide were monitored. The absorption changes of fluorophore **GSB** and **RSB** in the presence and absence of cyanide ion were displayed in **Figure 3.8**. In case of **GSB** probe, upon the addition of 100 equivalent of cyanide ion (1 mM), the maxima absorption peak at 504 nm disappeared and the new absorption peak at 345 nm was formed (**Figure 3.8, left**). Based on these results, we decided to use the A_{345}/A_{504} ratio to quantify the absorption changed in this system. Before the addition of cyanide ion, A_{342}/A_{504} of **GSB** was 0.2, and the addition of cyanide ion resulted in the increase of A_{342}/A_{504} to 11 which was 55-fold. This observation were corresponded with the color change which observed by naked eye. The orange color of **GSB** probe was decolorized and turned to colorless (**Figure 3.8, left, inset**). Similarly, before addition of cyanide ion, the **RSB** displayed the maxima absorption peak at 557 nm. Upon addition of cyanide ion (1mM), there was the new increased peak at 345 nm and the decreased peak at 557 nm (**Figure 3.8, right**). When we used the A_{345}/A_{557} ratio to quantify the absorption changed, approximately 5-fold increase was observed in the present of cyanide. Interestingly, the color change of **RSB** probe was visualized as decolorization from purple to colorless (**Figure 3.8, right, inset**). The results clearly demonstrated that **GSB** and **RSB** could be used as the naked-eye observation for cyanide sensing.

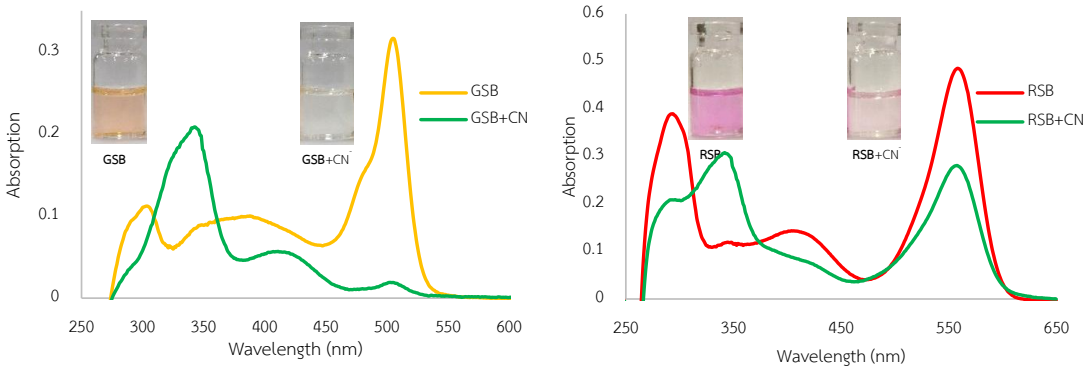

Figure 3.8 Absorption spectra of the solution of **GSB** (left) and **RSB** (right) (10μM) upon addition of sodium cyanide (1 mM) in 90% DMSO/TRIS buffer pH 7.4.

In case of fluorescence sensing ability for probe **GSB** and **RSB** toward cyanide ion, the fluorescence response were displayed in **Figure 3.9**. When excited at 345 nm, **GSB** enhanced the fluorescence emission at 504 nm upon the addition of 100 equivalent of cyanide ion (1 mM) (**Figure 3.9, left**). The fluorescence enhancement ratio (I/I_0) was found to be 46-fold. Moreover, we observed the strong green emission of **GSB** under black light upon the addition of cyanide as seen in **Figure 3.9** (**left, inset**). In term of quantum efficiency, upon the addition of CN^-, it change from 1% to 22%. On the other hand, the response of the **RSB** showed the different behavior. Upon the addition of 100 equivalent of cyanide ion (1 mM), **RSB** exhibited a prominent fluorescence enhancement accompanied by blue shift of 53 nm from 557 to 504 nm (**Figure 3.9, right**). This resulted in the flurogenic change from red to green emission (**Figure 3.9, right, inset**). Therefore we decided to use the ratiometric emission wavelength at 600 and 504 nm to quantify the enhancement efficiency. It showed the value of I_{600}/I_{504} before and after addition of CN^- were calculated to be 45-fold. These results suggested that **GSB** probes is promising as the fluorescence turn-on sensor for cyanide detection. On the other hand, **RSB** could serve as ratiometric fluorescence sensor for cyanide detection.

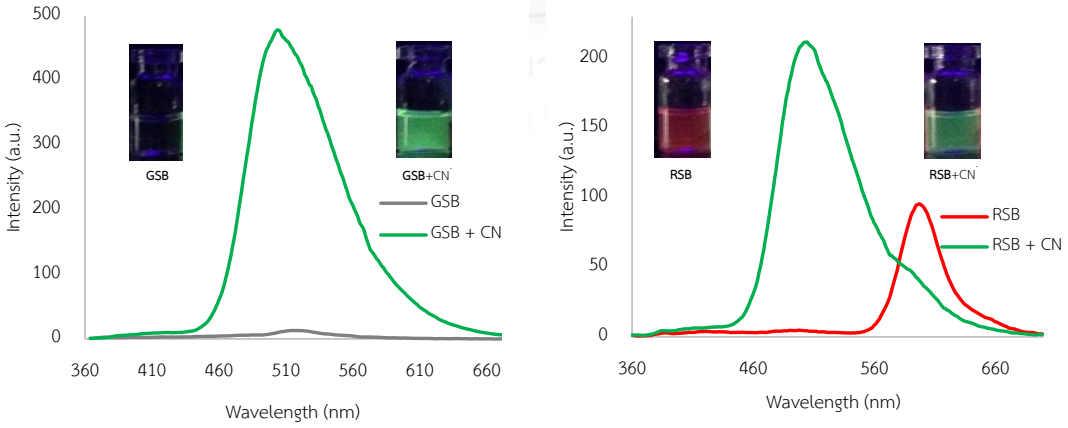

Figure 3.9 Emission spectra of the solution of **GSB** (left) and **RSB** (right) (10μM) upon addition of sodium cyanide (1mM) in 90% DMSO/TRIS buffer pH 7.4.

3.2 Sensitivity of GSB and RSB toward cyanide

With the optimized condition in hands, the absorption intensity in relationship to cyanide concentration was investigated upon addition of various equivalent of sodium cyanide (10-90 equivalents) in aqueous solvent (90% DMSO/TRIS buffer pH 7.4). For **GSB** probe, the absorption peak at 504 nm was dramatically decreased along with the increased of peak 345 nm (**Figure 3.10, left**). We also observed the gradual color change from orange to colorless solution upon the addition of cyanide. Similar to **GSB**, **RSB** displayed the decrease of absorption band at 557 nm with the increase of peak at 345 nm upon the addition of sodium cyanide (**Figure 3.10, right**). Moreover, the colorimetric change from purple to colorless was observed.

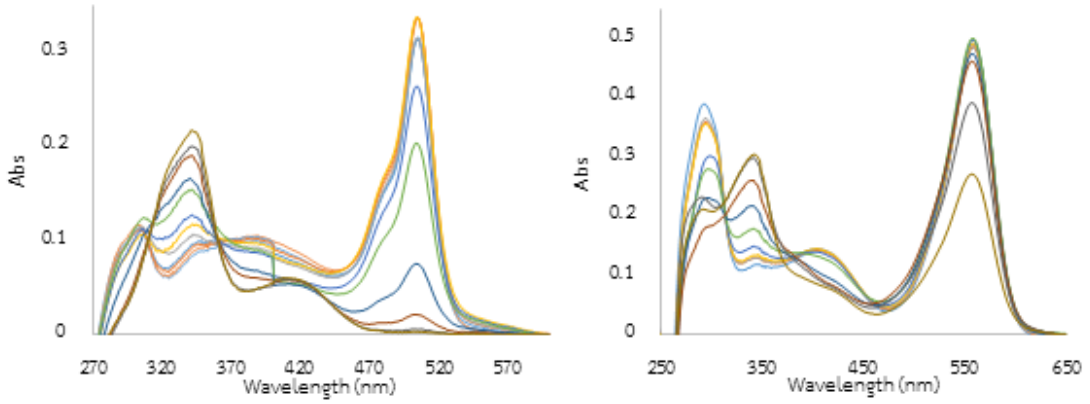

Figure 3.10 Absorption spectra change of the solution of **GSB** (left) and **RSB** (right) (10μM) upon addition of various sodium cyanide (1-70eqiv) in 90% DMSO/TRIS buffer pH 7.4.

For fluorescence change, **GSB** alone displayed weak fluorescence emission intensity at 529 nm while **RSB** displayed red fluorescence emission intensity at 557 nm. When we changed the excitation wavelength to the new absorption at 345 nm, upon addition of various equivalent of sodium cyanide from 1 – 90 equivalent led to the fluorescence enhancement significantly. In case of **GSB.** The strong green fluorescence emission was observed upon addition of sodium cyanide (**Figure 3.11, b left**). For the **RSB**, on the other hand, the ratiometric change was observed (**Figure 3.11, a right**). The peak at 600 nm was decreased graduately along with the increase

of peak at 504 nm. Under the black light, we saw the flurogenic change from red to green (**Figure 3.11, b right**). Moreover, the plot I/I_0 vs. concentration of cyanide of both **GSB** and **RSB** demonstrated that the fluorescence enhancement ratio could not reach the equilibrium point even though 90 equivalent of cyanide ion were added (**Figure 3.11, a and b inset**). These suggested that the fluorescence change of our sensor are the reaction mode.

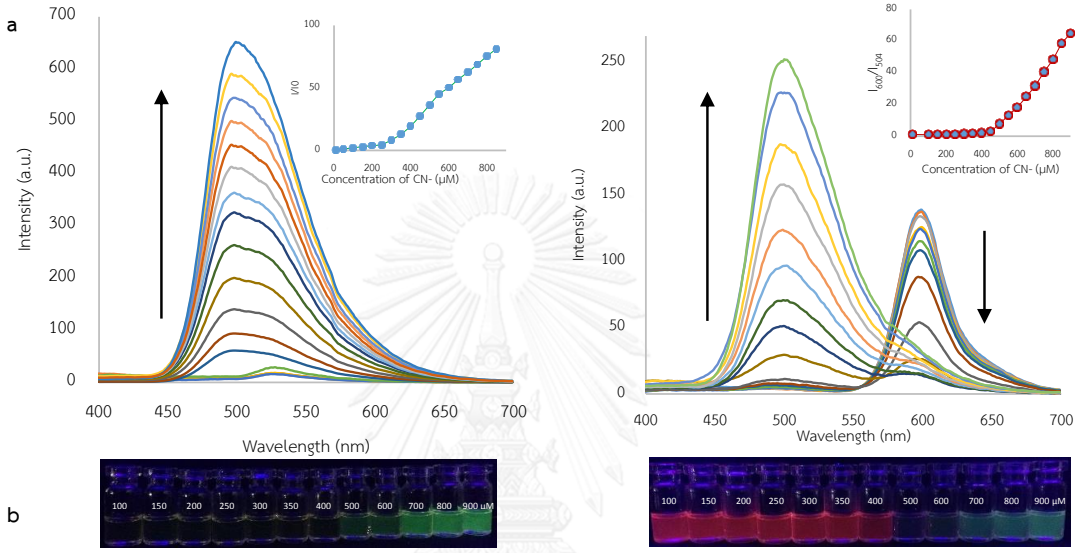

Figure 3.11 Emission spectra change (a) and visual observation under black light (b) of the solution of **GSB** (left) and **RSB** (right) (10μM) upon addition of various sodium cyanide (1-90eqiv) in 90% DMSO/ TRIS buffer pH 7.4.

As previous discussed, the fluorophore **RSB** exhibited ratiometric change from red to green with cyanide in TRIS buffer pH 7.4. Next, in order to improve the initial fluorescence intensity of **RSB**, the effect of surfactants was investigated. Varity of surfactants such as cationic (CTAB, DTAB, HTAB and TTAB), anionic (SDS, SDC, SDBS) and nonionic (TWEEN 20, Triton X-100 and Brij) surfactants were added to the **RSB** in 90% DMSO/ TRIS buffer pH 7.4 and the emission of RSB were showed in **Figure 3.12**. There were no significant change upon the addition of surfactants and 90% DMSO/ TRIS buffer pH 7.4 remained the best choice of this system.

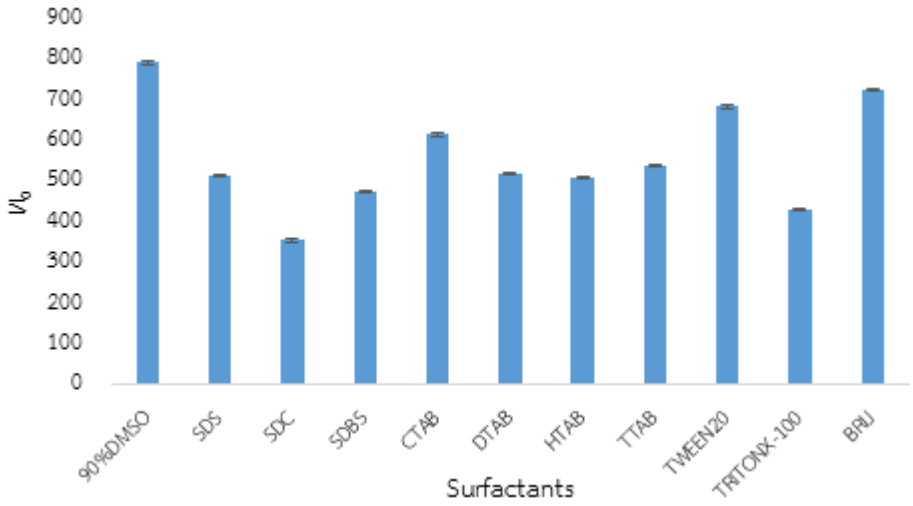

Figure 3.12 Bar chart representing the fluorescence enhancement (I/I_0) of **RSB** (10μM) in TRIS buffer pH 7.4 in the present of various surfactants (10mM). The fluorescence intensity at the emission peak of each system was used.

The time dependent studies of fluorescence response of both fluorophores in relationship to the amount cyanide were tested. Upon the addition of 100 equivalent of cyanide, the fluorescence intensity sharply increased during 0 – 60 min. And then the fluorescence intensity remained constantly throughout the entire experiment (320 min). This suggest that, reaction need around 60-70 min to consume all the cyanide ion (**Figure 3.13**). Also, this behavior confirm that the sensing mechanism is the reaction mode which we will explain more details in the next section.

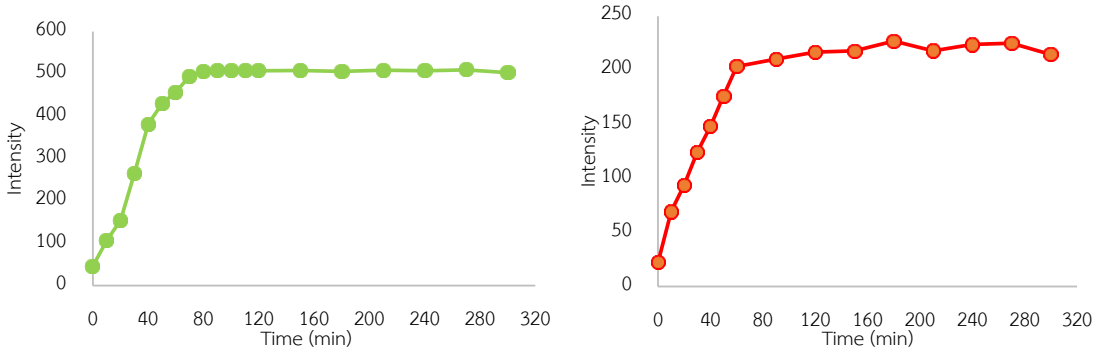

Figure 3.13 Time dependent changes in fluorescence intensity of **GSB** (left) and **RSB** (right) (10μM) upon addition of cyanide 100 equivalent in 90% DMSO/ TRIS buffer pH 7.4.

Even though the pH at 7.4 is an ideal for the fluorescence sensor, we also investigated the pH dependent of RSB fluorophore toward the fluorescence intensity in the absent of cyanide (**Figure 3.14**). Under the acidic condition (below pH 6.4), we found that the emission of **RSB** fluorophore was totally suppressed. This result perhaps governed by deprotonation at aldehyde moiety enhancing the ICT effect. On the other hand, in pH range between 6.4 - 8.4, **RSB** fluorophore exhibited the fluorescence intensity in the same range (365 – 493 a.u.). This suggest that our fluorophore are stable in the physical condition.

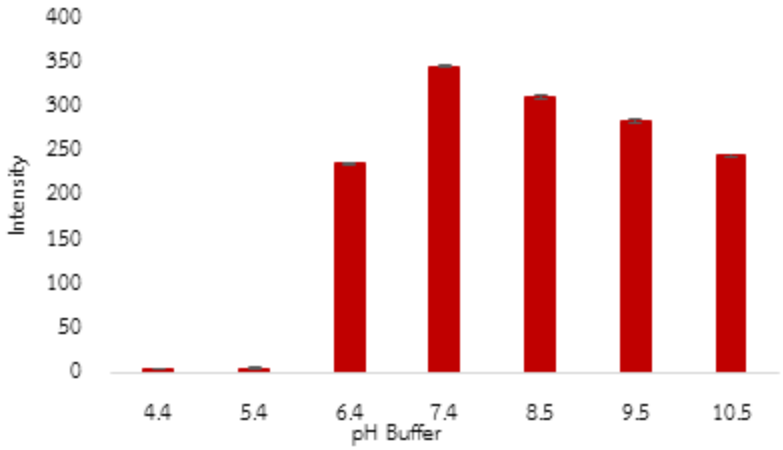

Figure 3.14 The fluorescence intensity of **RSB** (10μM) in 90%DMSO/ buffer pH 4.4 – 10.5.

3.3 Determination of detection limit of GSB and RSB toward cyanide

The detection limit was estimated by a plot of **Δ**I at 504 nm versus cyanide concentration in the range of 2-10 μM (**Figure 3.15**). The fluorescence enhancement ratio of **GSB** and **RSB** showed a well-behaved linear correlation in the studied range. The plot also gave the detection limit (at 3 x noise) of **GSB** and **RSB** cyanide sensing in the value of 0.88 and 1.79 μM, respectively. These values are lower than the WHO guideline (2.7 μM or 0.07mg/L) for cyanide allowed in fresh water. Therefore, our fluorophores are able to use for cyanide detection in aqueous system.

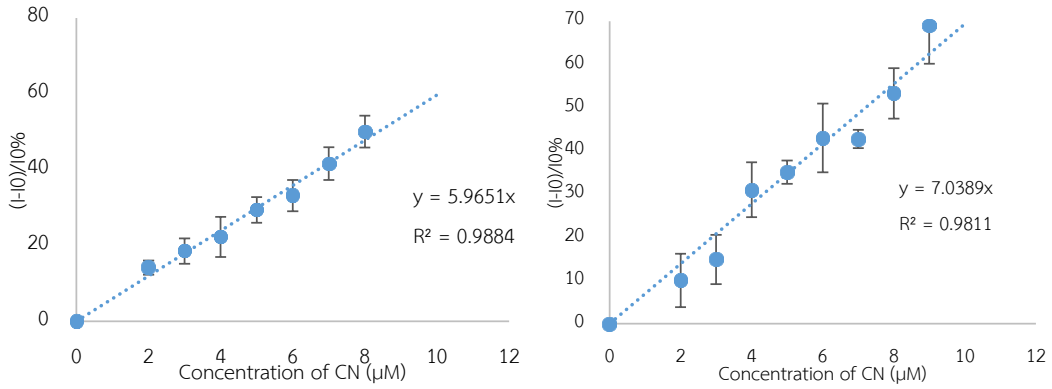

Figure 3.15 A plot of the fluorescence intensity change ($(I-I_0)/I_0$ x 100) of **GSB** (left) and **RSB** (right) (10μM) versus [CN^-]. (λ_{ex} = 345 nm; λ_{ex} = 504 nm; Medium = 90%DMSO/ TRIS buffer 7.4; [**F0**] = 1μM)

For the purposed mechanism of fluorescence enhancement of **GSB** and **RSB** toward cyanide ion. Initially, both of these probes has the ICT process along with the PET process that suppress the fluorescent emission as seen in **Figure 3.16 top**. We hypothesized that, at initial state, **GSB** was in deprotonated form due to the effect of electron withdrawing from BODIPY core. These resulted in the lower pKa of salicylaldehyde group (ca.8) under our tested condition (pH buffer 7.4). In attempt to gain more information of these phenomenal, structural optimization of **GSB** was carry out by DFT calculation in D88-LYP level as **Figure 3.16 below**. The optimized structure of **GSB** has extended **π**-conjugation between BODIPY core and salicylaldehyde thought the c-c triple bond linkage. HOMO of GSB was delocalized on BODIPY core while LUMO was delocalized on salicylaldehyde group. These suggest that the photo-induce electron transfer (PET) process between BODIPY and salicylaldehyde resulting in the fluorescence quenching of initial **GSB**. Upon the addition of the CN, it underwent nucleophilic attack to salicylaldehyde group and generated the cyanohydrin (**Figure 3.16, top, right**). Under pH buffer 7.4, the cyanohydrin could be exist in the protonated form due to the loss of aldehyde group. This would increase the pKa value of phenolic group close to the normal phenol (ca.9). Therefore the PET process from phenolate to BODIPY unit should be destroyed. Moreover, the structure optimization of cyanohydrin displayed that electron were delocalized in BODIPY unit in both of LUMO

and HOMO (**Figure 3.16, below, right**). Therefore, the attack of cyanide ion not only cause the change in pKa of phenolic group but also interrupt the **π**-conjugation causing the fluorescence enhancement of **GSB**.

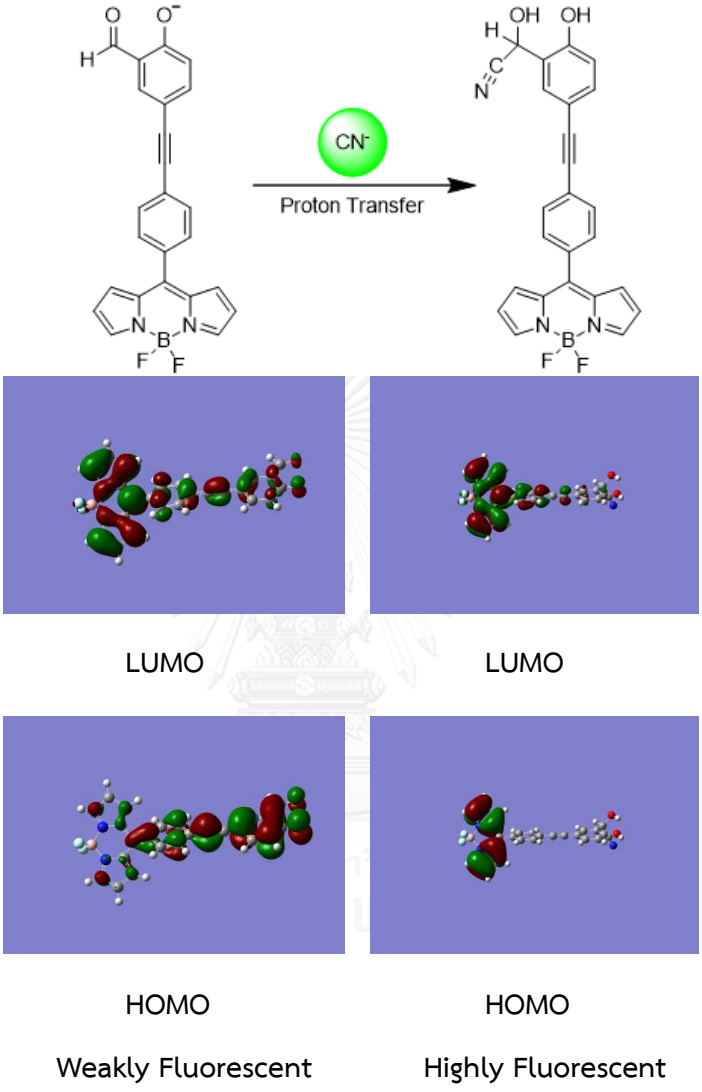

Figure 3.16 Purposed mechanism sensing of **GSB** toward cyanide ion.

The ^{1}H-NMR titration study of **RSB** in DMSO-d_6, it found that when addition of sodium cyanide 0.2 – 1.0 equivalent the peak of aldehyde at 11.14 ppm were disappeared while peat at 5.63 ppm were increased continuously (**Figure 3.17**). We discussed that the new peak is belong to the H at the cyanohydrin intermediate (**RSB –** CN) resulting from the attack of cyanide at aldehyde group (**Figure 3.17, top**).

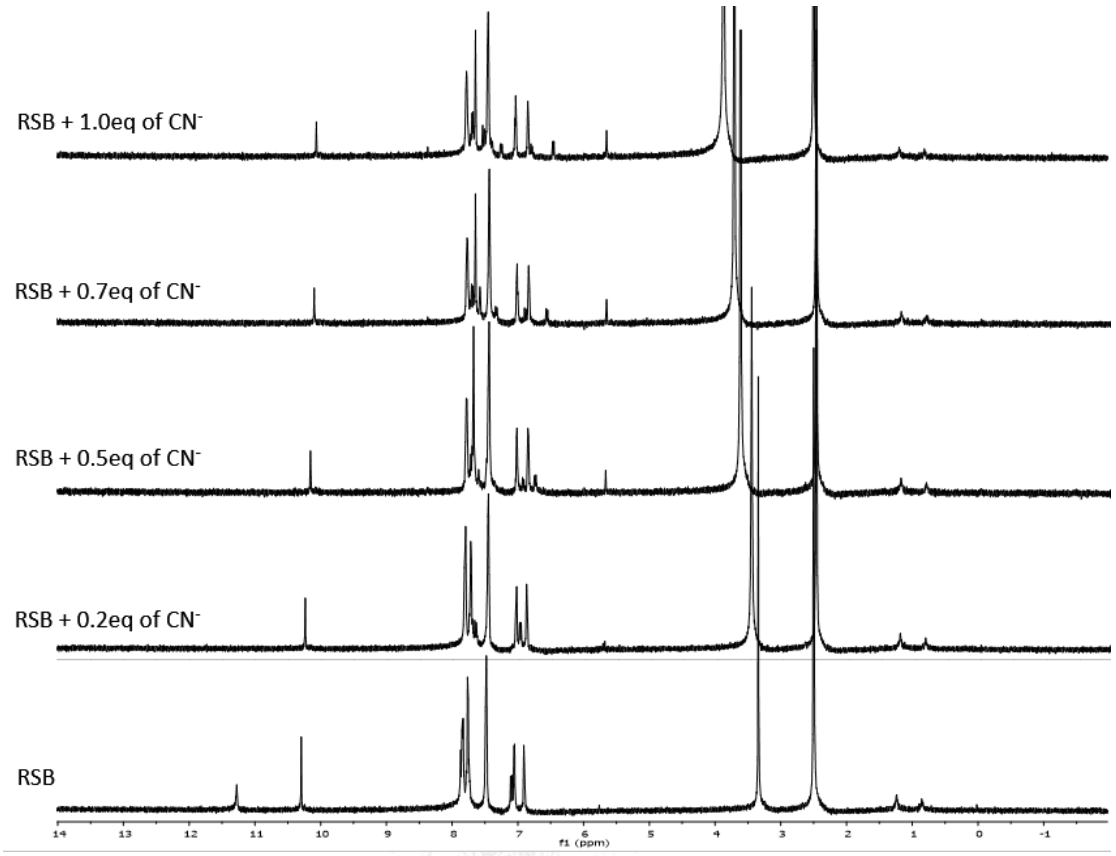

Figure 3.17 1H NMR Titration of **RSB** toward cyanide ion in DMSO-d_6

To investigate the selectivity of our sensors, cyanide and other 13 anions (SCN^-, HCO_3^-, OAc^-, NO_2^-, NO_3^-, F^-, Cl^-, Br^-, I^-, $S_2O_3^{2-}$, SO_3^{2-}, SO_4^{2-}, N_3^-) were tested with **GSB** and **RSB**. In **Figure 3.18**, **GSB** displayed high specificity and there was only cyanide ion can lower the absorption peak at 504 nm. This result caused the colorimetric change from orange to colorless with only cyanide ion (**Figure 3.18, c**). Even though absorption peak at 345 nm increased upon the addition of some anions (OAc^-, F^-, SO_2^{2-} and SO_3^{2-}) (**Figure 3.18, a)**, but the color of their solution remain unchanged. Therefore we decided to use the absorption ratio between 345 and 504 nm for quantified the naked eye observation. Ratio bars of A_{345}/A_{504} showed an approximately 55-fold enhancement in the present of cyanide ion in comparison with other 13 anions in case of **GSB** (**Figure 3.18, b**). Similarly, **RSB** showed high specificity to cyanide ion and absorption peak at 557 nm decreased along with the increase at 345 nm (**Figure 3.19, a**). This resulted in

the decolorized from purple to colorless (**Figure 3.19, c**) and the A_{345}/A_{557} ratio bars showed an approximately 5-fold increase after addition of cyanide ion (**Figure 3.19, b**).

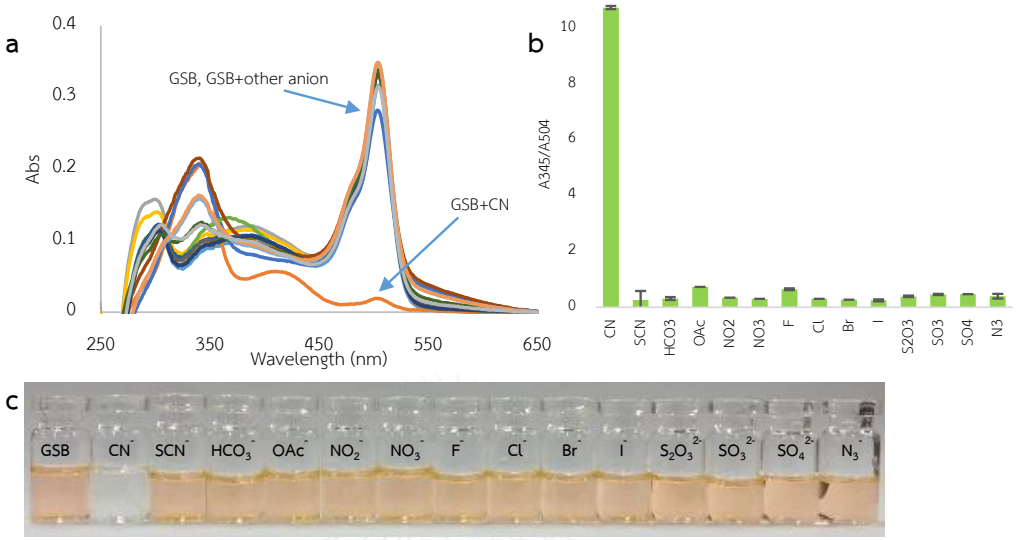

Figure 3.18 The Absorption spectra (a), A_{345}/A_{504} bar charts (b) and visual observation (c) of **GSB** upon addition of 14 common anions (CN^-, SCN^-, HCO_3^-, OAc^-, NO_2^-, NO_3^-, F^-, Cl^-, Br^-, I^-, $S_2O_3^{2-}$, SO_3^{2-}, SO_4^{2-}, N_3^-). (λ_{ex} = 345 nm; Medium = 90%DMSO/ TRIS buffer 7.4; [**GSB**] = 10μM; [anion] = 1 mM)

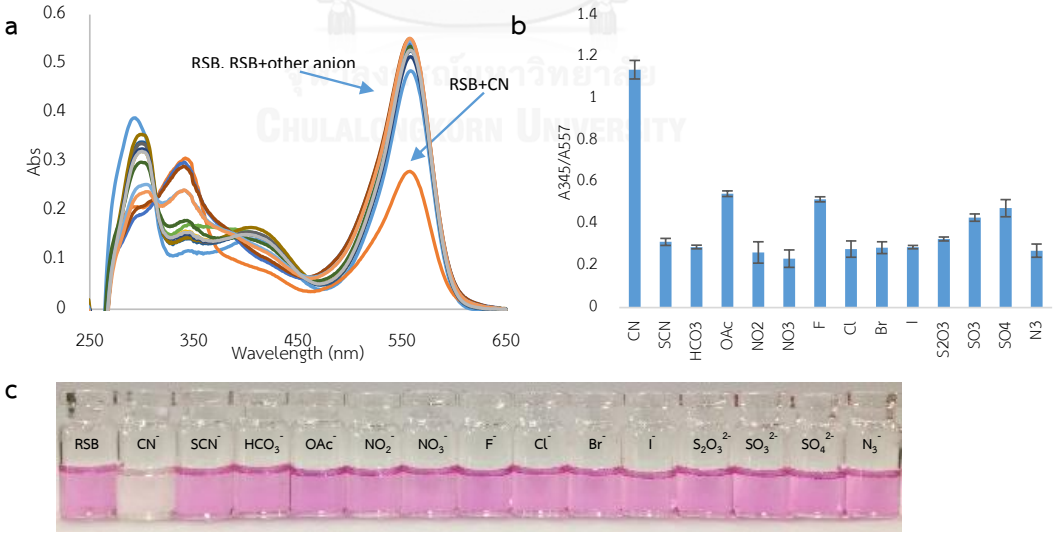

Figure 3.19 The Absorption spectra (a), A_{345}/A_{557} bar charts (b) and visual observation (c) of **RSB** upon addition of 14 common anions (CN^-, SCN^-, HCO_3^-, OAc^-, NO_2^-, NO_3^-, F^-, Cl^-, Br^-, I^-, $S_2O_3^{2-}$, SO_3^{2-}, SO_4^{2-}, N_3^-). (λ_{ex} = 345 nm; Medium = 90%DMSO/ TRIS buffer 7.4; [**RSB**] = 10μM; [anion] = 1 mM)

For the fluorescence selectivity tests, after the addition of anions to **GSB** solutions, it demonstrated the fluorescence enhancement of peak at 504 nm with only cyanide (**Figure 3.20, a**). Moreover the strong green emission were appeared under black light as seen on **Figure 3.20, c**. The emission enhancement ratio (I/I_0) bar showed 46-fold enhancement when compare to other 13 anions (**Figure 3.20, b**).

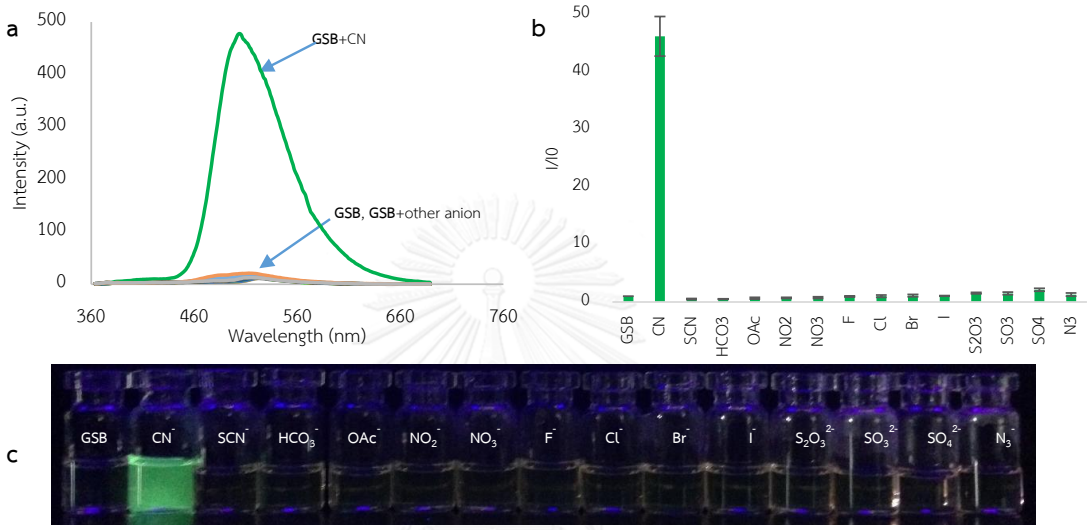

Figure 3.20 The fluorescence spectra (a), I/I_0 bar chart (b) and visual observation under black light (c) of **GSB** upon addition of 14 common anions (CN^-, SCN^-, HCO_3^-, OAc^-, NO_2^-, NO_3^-, F^-, Cl^-, Br^-, I^-, $S_2O_3^{2-}$, SO_3^{2-}, SO_4^{2-}, N_3^-). (λ_{ex} = 345 nm; Medium = 90%DMSO/ TRIS buffer 7.4; [**GSB**] = 10μM; [anion] = 1 mM)

On the other hand, in the present on cyanide, **RSB** exhibited the shift in the emission maxima from 557 to 504 nm (**Figure 3.21, a**). This resulted in the color change from red to green under the black light (**Figure 3.21, c**). Unlike cyanide, other anion such as OAc^- and F^- can also quench the emission signal at 557 nm but are not able to increase the emission signal at 504 nm. The emission enhancement ratio at 504 versus 600 nm was used to quantify the sensing abilities of **RSB** as showed in **Figure 3.21, b.** For cyanide ion, the ratio between I_{504}/I_{600} was 45-fold different from the other anions. Based on these results, **GSB** and **RSB** can be used for specific fluorescence turn-on and colorimetric sensor for visual detection of CN^- over competitive anions.

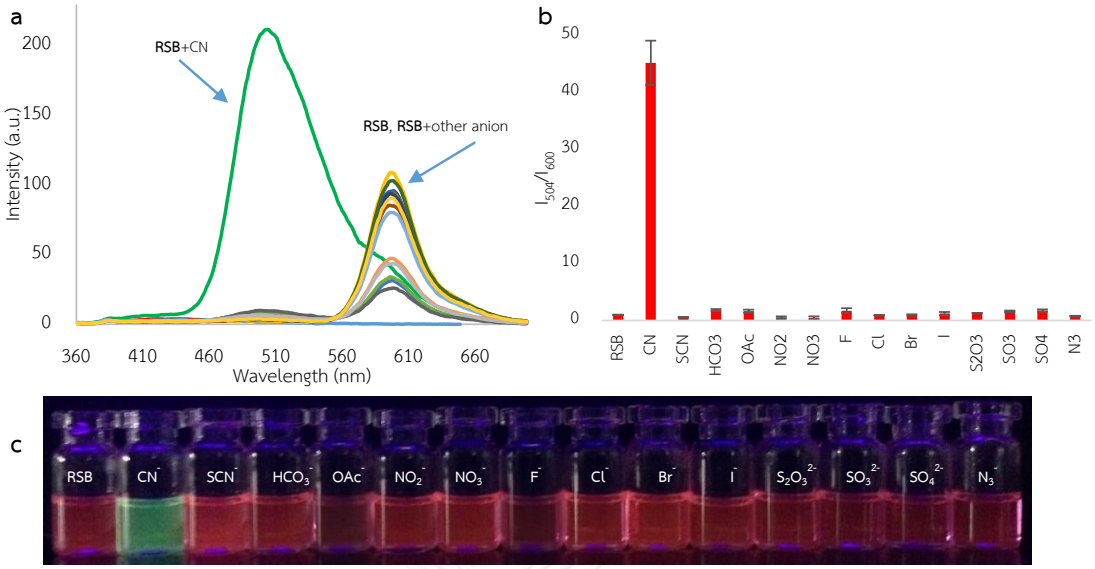

Figure 3.21 The fluorescence spectra (a), I/I_0 bar chart (b) and visual observation under black light (c) of **RSB** upon addition of 14 common anions (CN^-, SCN^-, HCO_3^-, OAc^-, NO_2^-, NO_3^-, F^-, Cl^-, Br^-, I^-, $S_2O_3^{2-}$, SO_3^{2-}, SO_4^{2-}, N_3^-). (λ_{ex} = 345 nm; Medium = 90%DMSO/TRIS buffer 7.4; [**RSB**] = 10μM; [anion] = 1 mM)

The competitive test was conducted by adding cyanide ion and another anion to the **GSB** or **RSB** solutions and the fluorescence response (I/I_0) were summarized in **Figure 3.22** and **Figure 3.23**. In the present of mixture of cyanide/other anions in 1:3 ratio, it reveal that they are no significantly different fluorescence intensity of the **GSB** and **RSB** (**Figure 3.22**) but did result in slight fluorescence quenching fir SCN^-. However when competitive anion were increase to 1:5 ratio, the SCN^- was strongly interfere causing completely quench in fluorescence signal. However, the quenching behavior from SCN^- could not be explain in yet but the mixture of fluorophore and cyanide could be used for SCN^- detection.

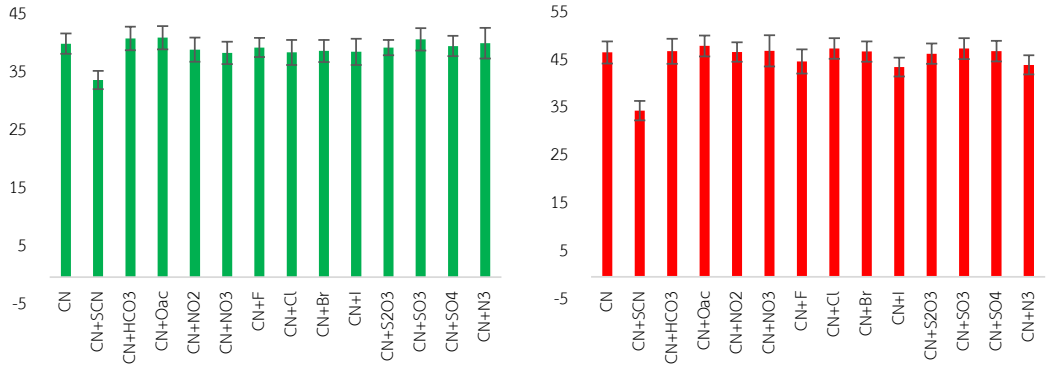

Figure 3.22 The bars represent the fluorescence enhancement ratio (I/I_0) of **GSB** (left) and **RSB** (right) upon addition of CN^- in the present of another 13 anions (SCN^-, HCO_3^-, OAc^-, NO_2^-, NO_3^-, F^-, Cl^-, Br^-, I^-, $S_2O_3^{2-}$, SO_3^{2-}, SO_4^{2-}, N_3^-). (λ_{ex} = 345 nm; Medium = 90%DMSO/TRIS buffer 7.4; [**GSB** and **RSB**] = 10μM; [CN^-] = 500 μM; [another anion] = 1.5 mM)

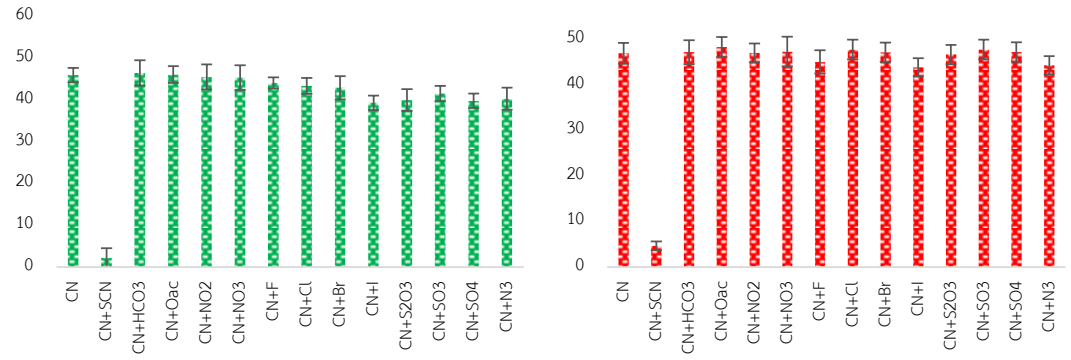

Figure 3.23 The bars represent the fluorescence enhancement ratio (I/I_0) of **GSB** (left) and **RSB** (right) upon addition of CN^- in the present of another 13 anions (SCN^-, HCO_3^-, OAc^-, NO_2^-, NO_3^-, F^-, Cl^-, Br^-, I^-, $S_2O_3^{2-}$, SO_3^{2-}, SO_4^{2-}, N_3^-). (λ_{ex} = 345 nm; Medium = 90%DMSO/TRIS buffer 7.4; [**GSB** and **RSB**] = 10μM; [CN^-] = 500 μM; [another anion] = 2.5 mM)

3.4 Application in cell imaging

Fluorescent probes & dyes in cellular biology have recently become the one of the most popular biological analysis due to, there is non-destructive way of tracking or analyzing biological molecules. Therefore, we tested the **GSB** and **RSB** as the fluorescence dye for the detection of cyanide in living cell. HepG2 cells were chose as example cell lines and fluorescence images were recorded under fluorescence microscope showing no fluorescence emission under green and red field (**Figure 3.24A**). After incubation of 0.5 μM of **GSB** and **RSB** for 30 min at 37 ^{o}C, the weak green emission was detected in case of **GSB** while **RSB** exhibited the strong red emission in cytoplasm of HepG2 cell. On the other hand, when 0.5 mM of NaCN were added to HepG2 cell for 1 hr at 37 ^{o}C and it was further incubated with **GSB** and **RSB**, it induced the strong green emission in case of **GSB** (**Figure 3.24E**) and flurogenic change from red to green in case of **RSB** (**Figure 3.24F**). These results suggested the ability to use the **GSB** and **RSB** as dyes for visualizing CN^{-} in living cell.

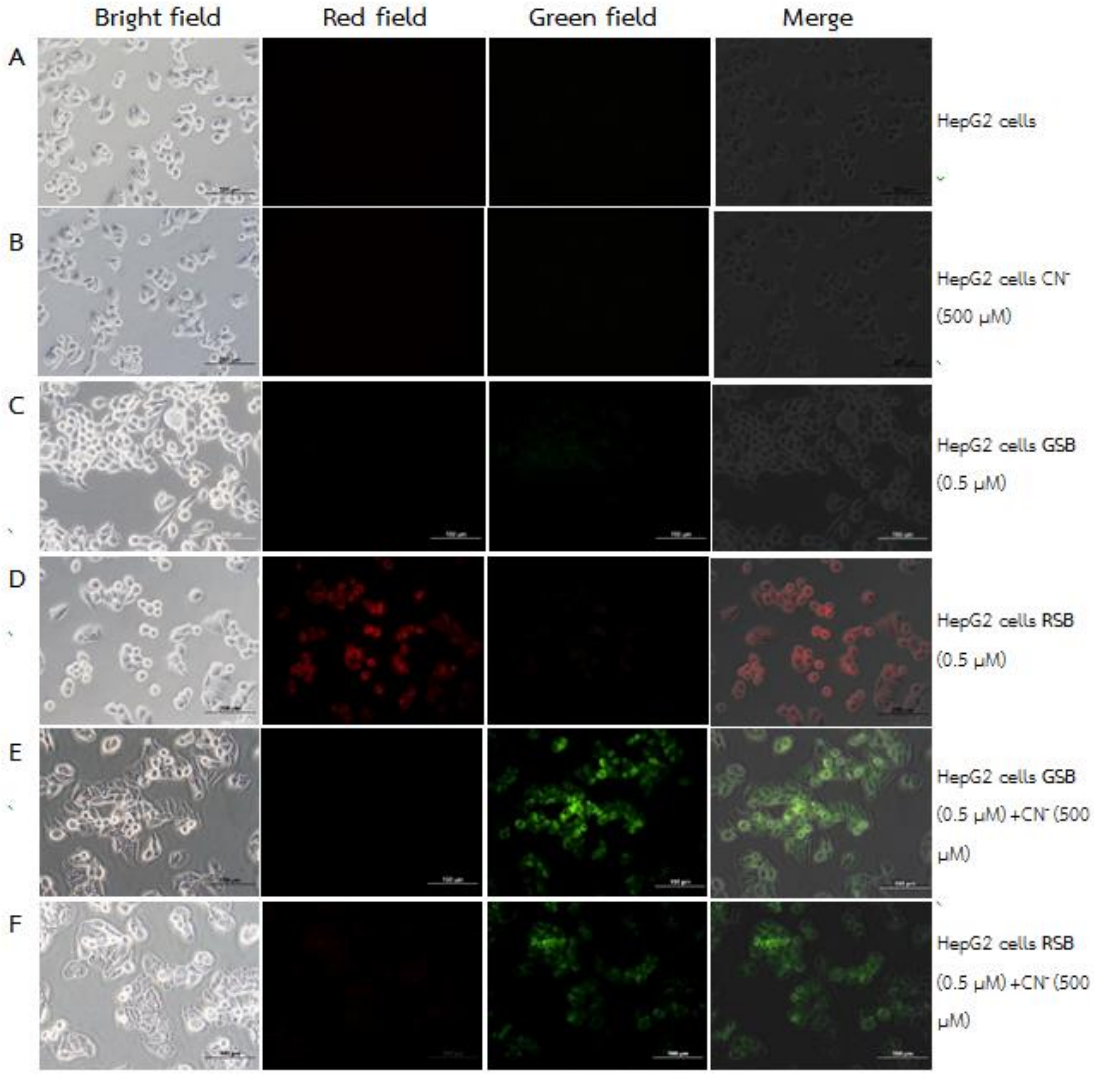

Figure 3.24 Bright and fluorescence images of HepG2 cells (A) (control), treated with 0.5 mM of sodium cyanide (B), incubated with 0.5 μM of **GSB** and **RSB** (C, D), treated with 0.5 mM of sodium cyanide then incubated with 0.5 μM of **GSB** and **RSB** (E, F).

CHAPTER IV

CONCLUSION

In summary, two new fluorophore **GSB** and **RSB** were successful synthesized from the sonogashira coupling reaction to introduce the BODIPY core connected to salicylaldehyde receptor. Both **GSB** and **RSB** probes can be used as naked eye sensor displaying highly selective and sensitive colorimetric change from orange and purple to colorless in the presence of cyanide anion. Moreover, **GSB** exhibited exclusive "off-on" green emission response while **RSB** demonstrated flurogenic change from red to green emission toward cyanide anion. The other 13 competitive anions did not show significant interference in visual observation. The detection limit of **GSB** and **RSB** probes were calculated to be 0.88 and 1.79 μM, respectively which are below the concentration limited by WHO in drinking water of 2.7 μM. The sensing mechanisms of two probes were investigated by density functional theory (DFT) calculation. Moreover, **GSB** and **RSB** were successfully extended to the intracellular cyanide detection which was confirmed by fluorescence microscopy imaging in HepG2 cell lines. The outcome of this research suggested that the sensing ability of **GSB** and **RSB** will make a great tool for cyanide detection in aqueous and living cell system as well as provide the key information for future fluorescence probe design.

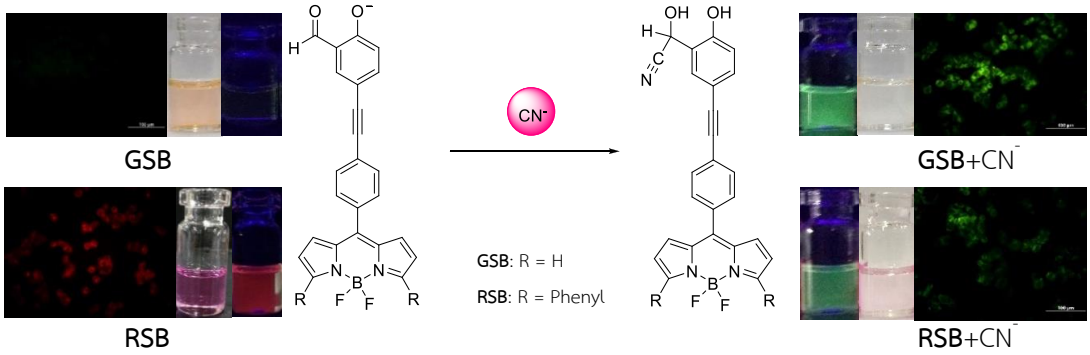

REFERENCES

[1] Long, L., Wang, L., and Wu, Y. A Fluorescence Ratiometric Probe for Detection of Cyanide in Water Sample and Living Cells. Chemistry & Materials Science 3(8) (2013): 307-313.

[2] Vetter, J. Plant cyanogenic glycosides. Toxicon 38(1) (2000): 11-36.

[3] Yang, L., Li, X., Yang, J., Qu, Y., and Hua, J. Colorimetric and Ratiometric Near-Infrared Fluorescent Cyanide Chemodosimeter Based on Phenazine Derivatives. ACS Applied Materials & Interfaces 5(4) (2013): 1317-1326.

[4] Jhong, Y., Hsieh, W., Chir, J.-L., and Wu, A.-T. A Highly Selective and Turn-on Fluorescence Sensor for Detection of Cyanide. Journal of Fluorescence 24(6) (2014): 1723-1726.

[5] Chen, C.-L., Chen, Y.-H., Chen, C.-Y., and Sun, S.-S. Dipyrrole Carboxamide Derived Selective Ratiometric Probes for Cyanide Ion. Organic Letters 8(22) (2006): 5053-5056.

[6] Long, L., et al. A highly selective and sensitive fluorescence ratiometric probe for cyanide and its application for the detection of cyanide in natural water and biological samples. Analytical Methods 5(23) (2013): 6605-6610.

[7] Organization, W.H. Guildlines for drinking-water quality World Health Organization 2004. Available from: http://www.who.int/water_sanitation_health/dwq/guidelines/en/

[8] Skoog, D.A., Holler, F.J., and Crouch, S.R. Fundamentals of Analytical Chemistry. 4 ed. New York: Saunders Collage Pubshing, 1982.

[9] Lakowicz, J.R. Principles of Fluorescence Spectroscopy. 3 ed.: John Wiley & Sons, Inc, 2006.

[10] Caballero, A., et al. Highly Selective Chromogenic and Redox or Fluorescent Sensors of Hg2+ in Aqueous Environment Based on 1,4-Disubstituted Azines. Journal of the American Chemical Society 127(45) (2005): 15666-15667.

[11] Tang, Y., et al. Direct Visualization of Glucose Phosphorylation with a Cationic Polythiophene. Advanced Materials 20(4) (2008): 703-705.

[12] McQuade, D.T., Pullen, A.E., and Swager, T.M. Conjugated Polymer-Based Chemical Sensors. Chemical Reviews 100(7) (2000): 2537-2574.

[13] Thomas, S.W., Joly, G.D., and Swager, T.M. Chemical Sensors Based on Amplifying Fluorescent Conjugated Polymers. Chemical Reviews 107(4) (2007): 1339-1386.

[14] Service, R.F. Chemistry Nobel - Getting a charge out of plastics. Science 290(5491) (2000): 425-+.

[15] Perepichka, I.F., Perepichka, D.F., Meng, H., and Wudl, F. Light-Emitting Polythiophenes. Advanced Materials 17(19) (2005): 2281-2305.

[16] Patil, A.O., Heeger, A.J., and Wudl, F. Optical properties of conducting polymers. Chemical Reviews 88(1) (1988): 183-200.

[17] Scherf, U. and List, E.J.W. Semiconducting Polyfluorenes—Towards Reliable Structure–Property Relationships. Advanced Materials 14(7) (2002): 477-487.

[18] Kraft, A., Grimsdale, A.C., and Holmes, A.B. Electroluminescent Conjugated Polymers—Seeing Polymers in a New Light. Angewandte Chemie International Edition 37(4) (1998): 402-428.

[19] Bunz, U.H.F. Poly(aryleneethynylene)s: Syntheses, Properties, Structures, and Applications. Chemical Reviews 100(4) (2000): 1605-1644.

[20] Chakraborty, A., Kar, S., Nath, D.N., and Guchhait, N. Photoinduced intramolecular charge-transfer reactions in 4-amino-3-methyl benzoic acid methyl ester: A fluorescence study in condensed-phase and jet-cooled molecular beams. Journal of Chemical Sciences 119(2) (2007): 195-204.

[21] Chattopadhyay, N., Serpa, C., Pereira, M.M., Seixas de Melo, J., Arnaut, L.G., and Formosinho, S.J. Intramolecular Charge Transfer of p-(Dimethylamino)benzethyne: A Case of Nonfluorescent ICT State. The Journal of Physical Chemistry A 105(44) (2001): 10025-10030.

[22] Chung, S.-K., Tseng, Y.-R., Chen, C.-Y., and Sun, S.-S. A Selective Colorimetric Hg2+ Probe Featuring a Styryl Dithiaazacrown Containing Platinum(II) Terpyridine Complex through Modulation of the Relative Strength of ICT and MLCT Transitions. Inorganic Chemistry 50(7) (2011): 2711-2713.

[23] Druzhinin, S.I., Mayer, P., Stalke, D., von Bülow, R., Noltemeyer, M., and Zachariasse, K.A. Intramolecular Charge Transfer with 1-tert-Butyl-6-cyano-1,2,3,4-tetrahydroquinoline (NTC6) and Other Aminobenzonitriles. A Comparison of Experimental Vapor Phase Spectra and Crystal Structures with Calculations. Journal of the American Chemical Society 132(22) (2010): 7730-7744.

[24] Galievsky, V.A., et al. Ultrafast Intramolecular Charge Transfer with N-(4-Cyanophenyl)carbazole. Evidence for a LE Precursor and Dual LE + ICT Fluorescence. The Journal of Physical Chemistry A 114(48) (2010): 12622-12638.

[25] Samori, S., Tojo, S., Fujitsuka, M., Spitler, E.L., Haley, M.M., and Majima, T. Donor–Acceptor-Substituted Tetrakis(phenylethynyl)benzenes as Emissive Molecules during Pulse Radiolysis in Benzene. The Journal of Organic Chemistry 72(8) (2007): 2785-2793.

[26] Xu, Z., Qian, X., and Cui, J. Colorimetric and Ratiometric Fluorescent Chemosensor with a Large Red-Shift in Emission: Cu(II)-Only Sensing by Deprotonation of Secondary Amines as Receptor Conjugated to Naphthalimide Fluorophore. Organic Letters 7(14) (2005): 3029-3032.

[27] Yoshihara, T., Druzhinin, S.I., and Zachariasse, K.A. Fast Intramolecular Charge Transfer with a Planar Rigidized Electron Donor/Acceptor Molecule. Journal of the American Chemical Society 126(27) (2004): 8535-8539.

[28] Zachariasse, K.A., Druzhinin, S.I., Bosch, W., and Machinek, R. Intramolecular Charge Transfer with the Planarized 4-Aminobenzonitrile 1-tert-Butyl-6-cyano-1,2,3,4-tetrahydroquinoline (NTC6). Journal of the American Chemical Society 126(6) (2004): 1705-1715.

[29] Galievsky, V.A. and Zachariasse, K.A. Intramolecular Charge Transfer with N,N-Dialkyl-4-(Trifluoromethyl)anilines and 4-(Dimethylamino)benzonitrile in Polar Solvents. Investigation of the Excitation Wavelength Dependence of the Reaction Pathway. Acta Physica Polonica A 112 (2007): 39-56.

[30] Spitler, E.L., Monson, J.M., and Haley, M.M. Structure–Property Relationships of Fluorinated Donor/Acceptor Tetrakis(phenylethynyl)benzenes and

Bis(dehydrobenzoannuleno)benzenes. The Journal of Organic Chemistry 73(6) (2008): 2211-2223.

[31] Li, J.-B., Hu, J.-H., Chen, J.-J., and Qi, J. Cyanide detection using a benzimidazole derivative in aqueous media. Spectrochimica Acta Part A: Molecular and Biomolecular Spectroscopy 133(0) (2014): 773-777.

[32] Niamnont, N., Khumsri, A., Promchat, A., Tumcharern, G., and Sukwattanasinitt, M. Novel salicylaldehyde derivatives as fluorescence turn-on sensors for cyanide ion. Journal of Hazardous Materials 280(0) (2014): 458-463.

[33] Loudet, A. and Burgess, K. BODIPY Dyes and Their Derivatives: Syntheses and Spectroscopic Properties. Chemical Reviews 107(11) (2007): 4891-4932.

[34] Boens, N., Leen, V., and Dehaen, W. Fluorescent indicators based on BODIPY. Chemical Society Reviews 41(3) (2012): 1130-1172.

[35] Liu, W., Tang, A., Chen, J., Wu, Y., Zhan, C., and Yao, J. Photocurrent Enhancement of BODIPY-Based Solution-Processed Small-Molecule Solar Cells by Dimerization via the Meso Position. ACS Applied Materials & Interfaces 6(24) (2014): 22496-22505.

APPENDIX

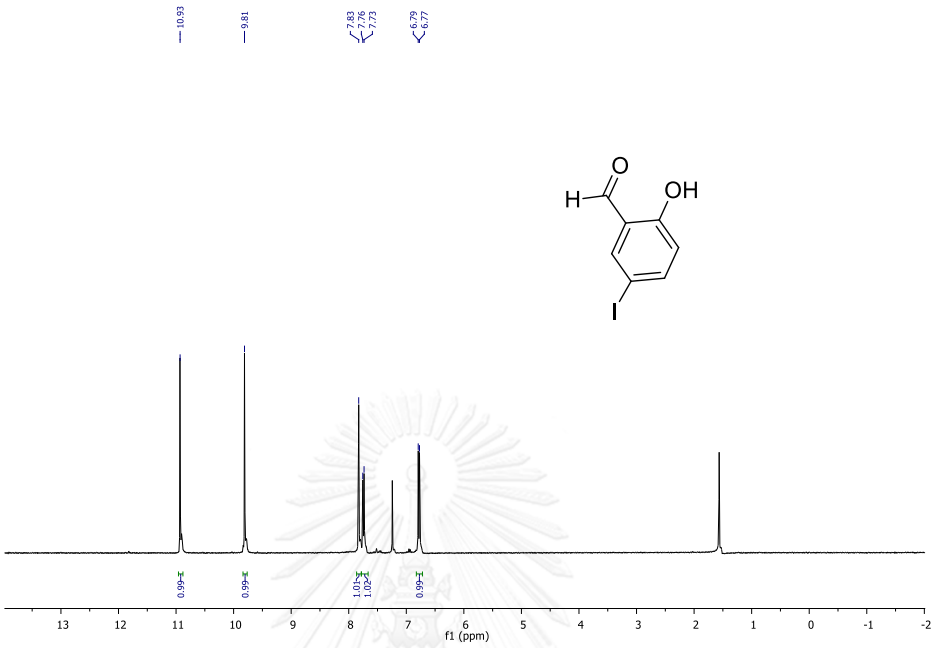

Figure S.1 ^{1}H-NMR spectrum of 2-Hydroxy-5-iodobenzaldehyde (**2**)

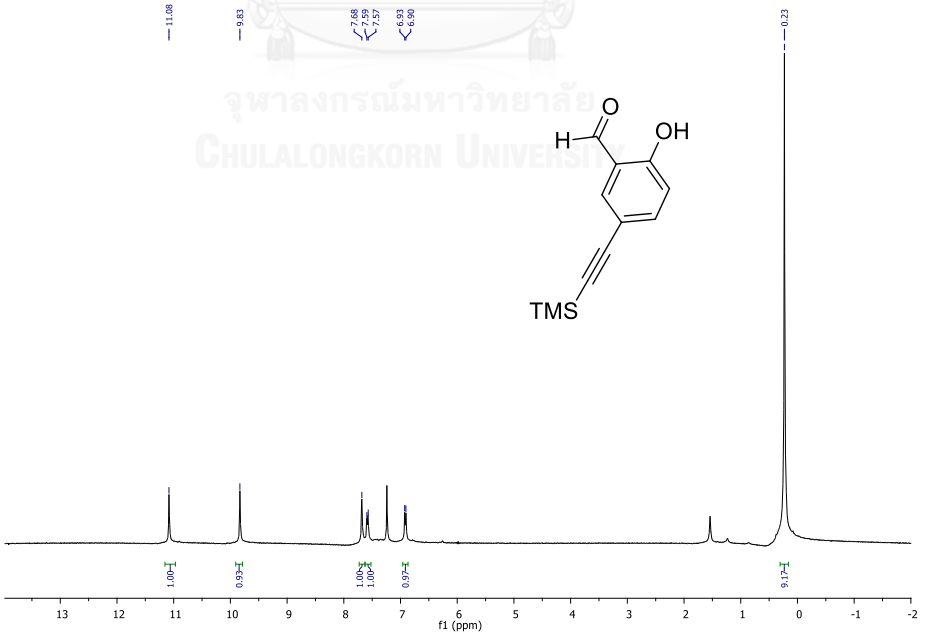

Figure S.2 ^{1}H-NMR spectrum of 2-Hydroxy-5-((trimethylsilyl)ethynyl)benzaldehyde (**3**)

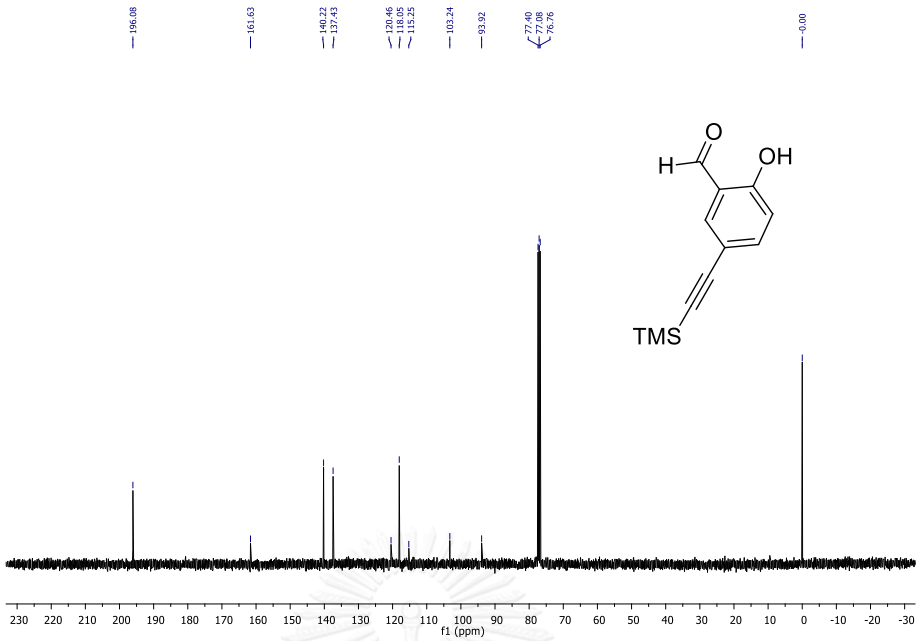

Figure S.3 ^{13}C-NMR spectrum of 2-Hydroxy-5-((trimethylsilyl)ethynyl)benzaldehyde (**3**)

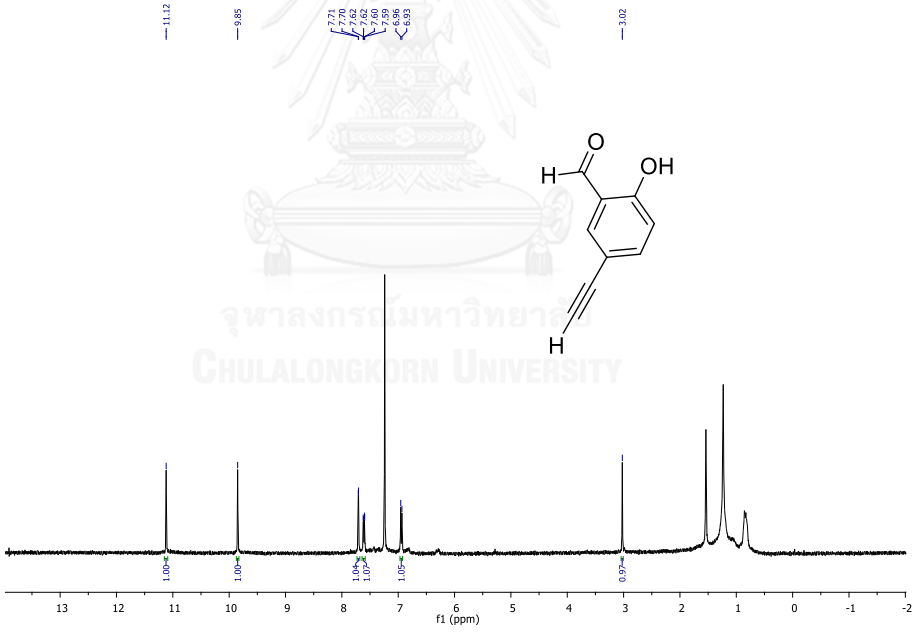

Figure S.4 ^{1}H-NMR spectrum of 5-ethynyl-2-hydroxybenzaldehyde (**4**)

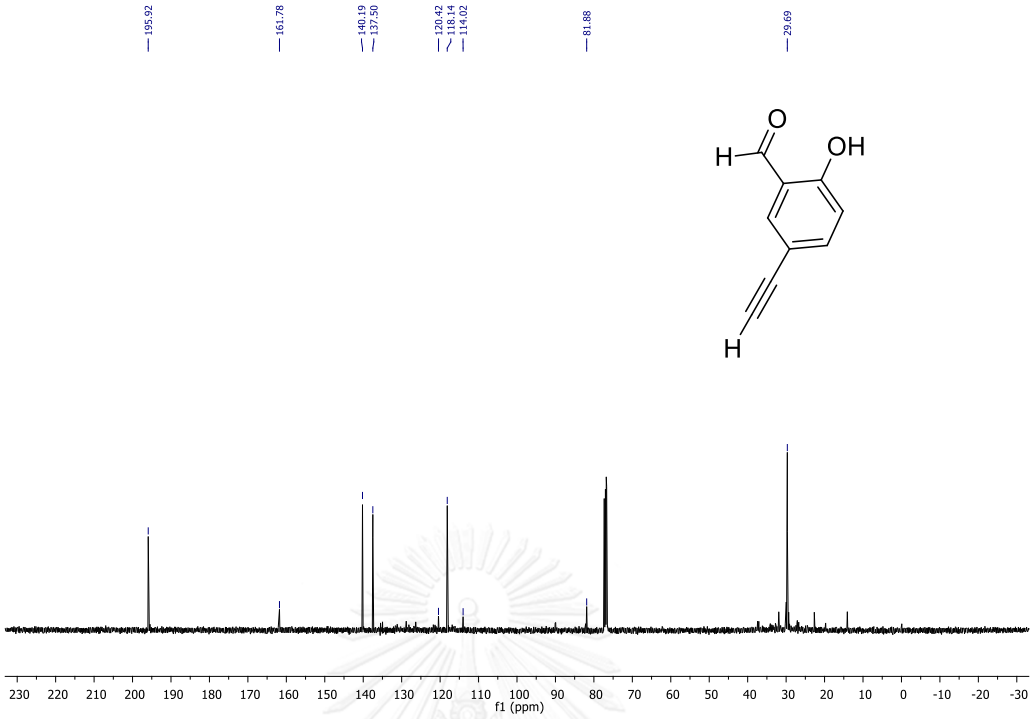

Figure S.5 ^{13}C-NMR spectrum of 5-ethynyl-2-hydroxybenzaldehyde (**4**)

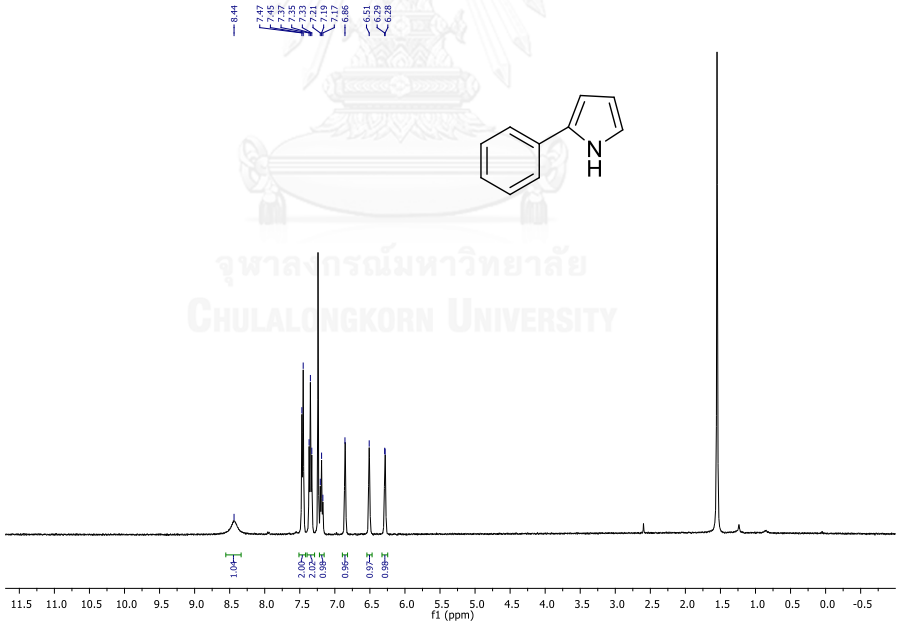

Figure S.6 ^{1}H-NMR spectrum of **6b**

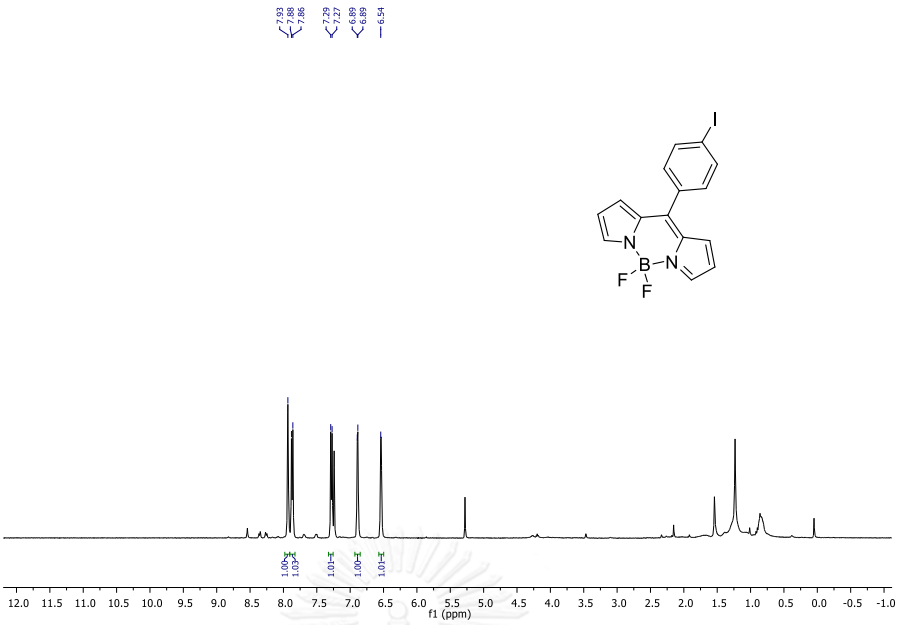

Figure S.7 ^{1}H-NMR spectrum of **7a** ((Solvent peak need attention!!

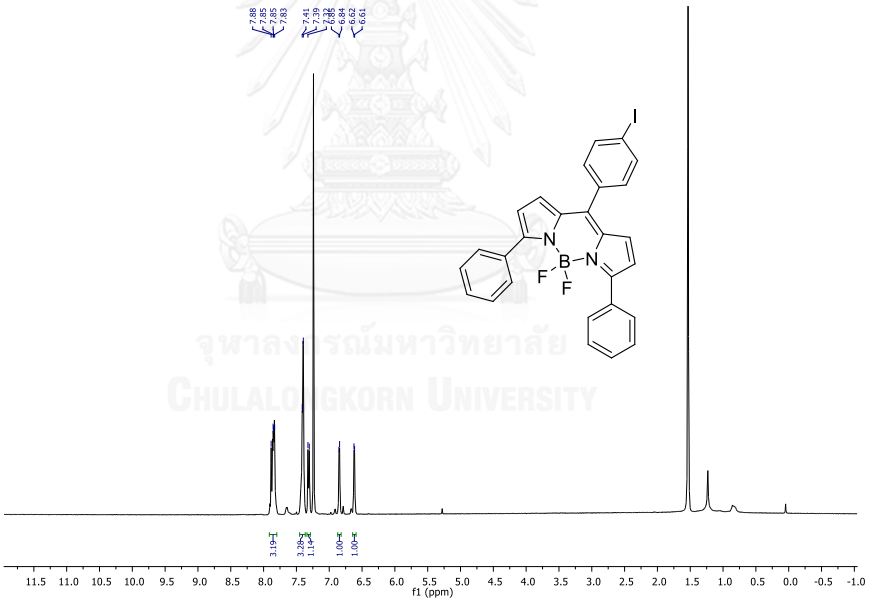

Figure S.8 ^{1}H-NMR spectrum of **7b**

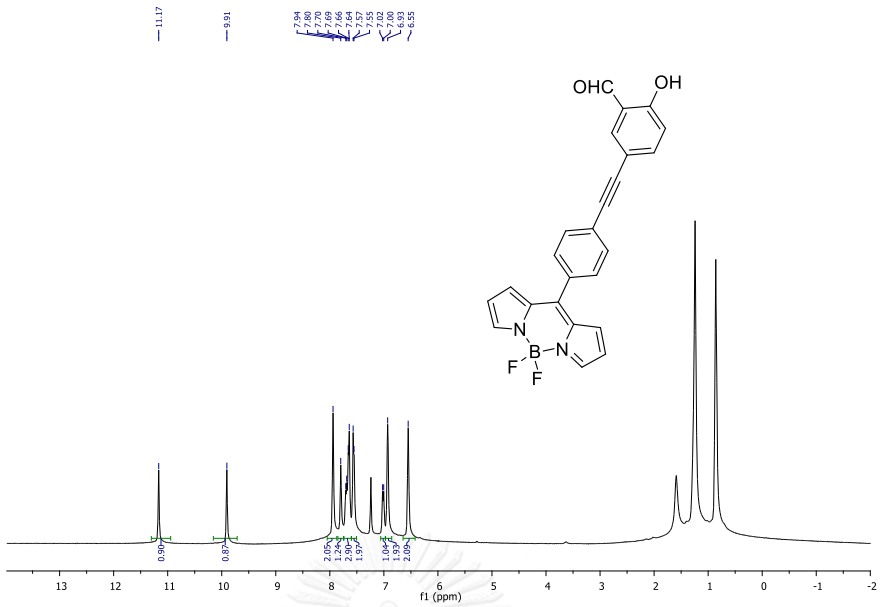

Figure S.9 ^{1}H-NMR spectrum of **GSB**

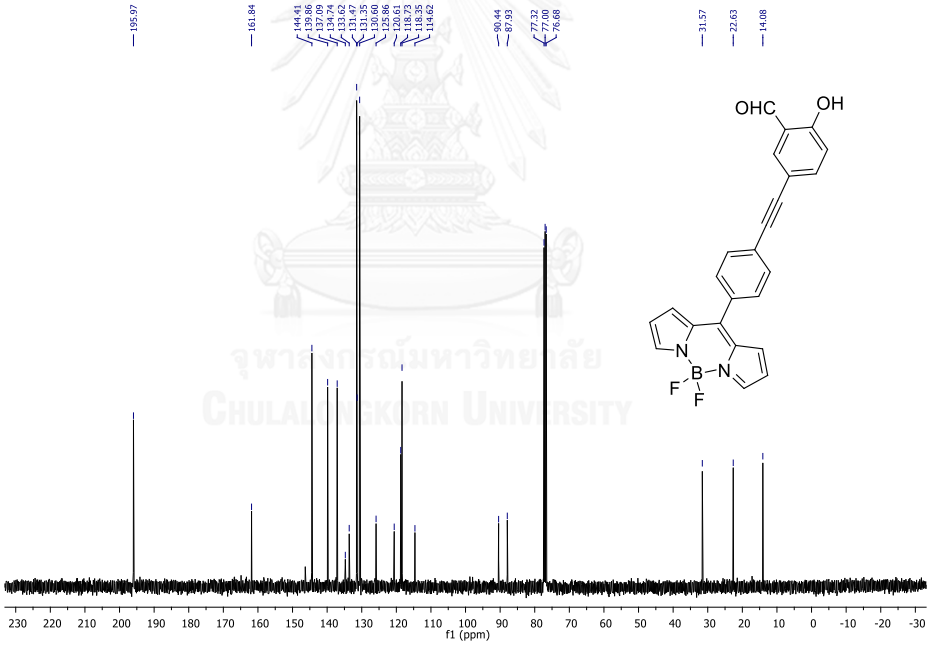

Figure S.10 ^{13}C-NMR spectrum of **GSB**

	Compound	Compound + Na^+	Found
GSB	412.1195	435.1092	435.1181

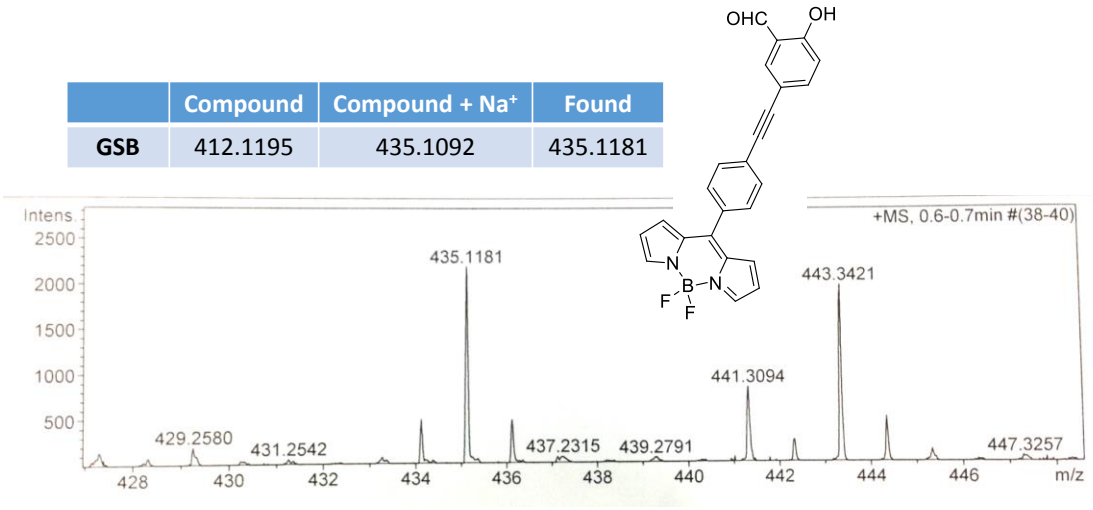

Figure S.11 Mass spectrum of **GSB**

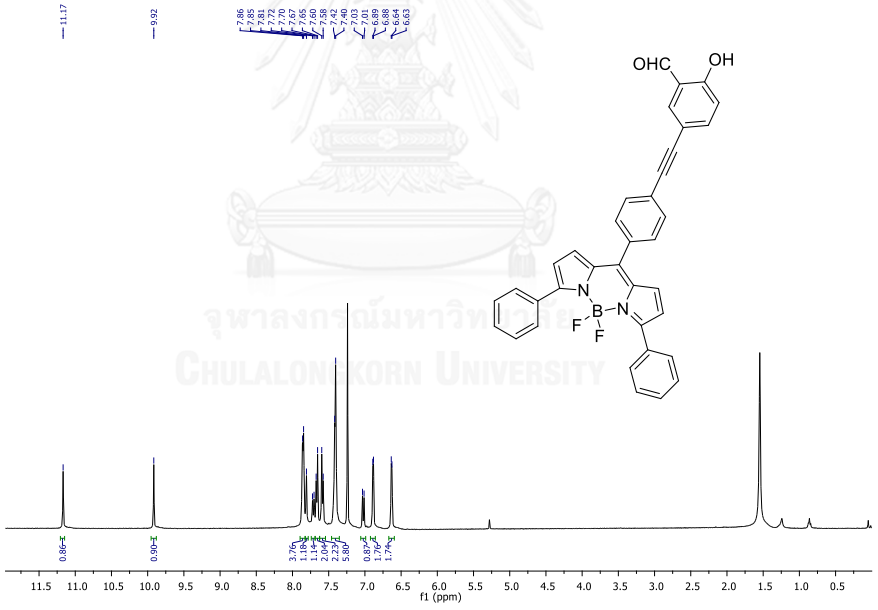

Figure S.12 ^{1}H-NMR spectrum of **RSB**

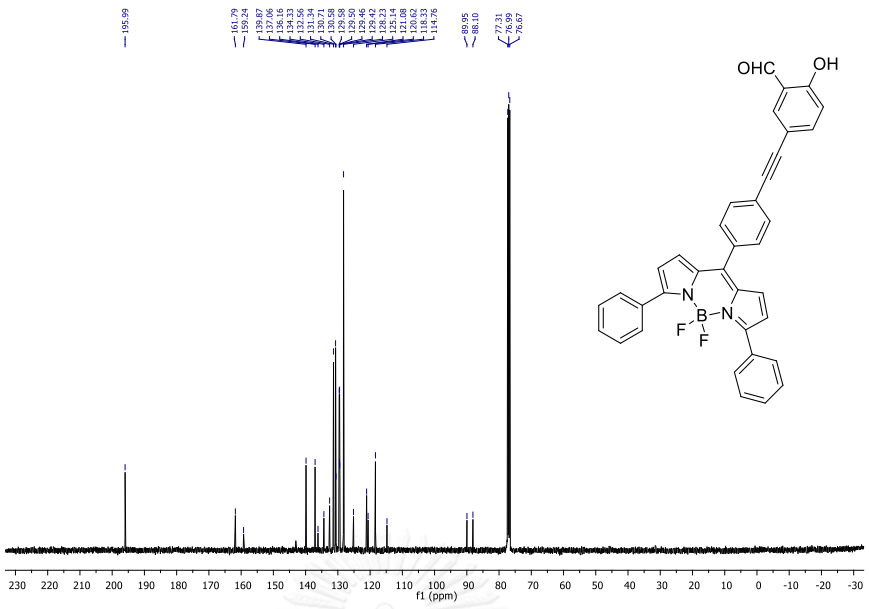

Figure S.13 ^{1}C-NMR spectrum of **RSB**

Compound	Compound + Na^+	Found
564.821	587.8107	587.1838

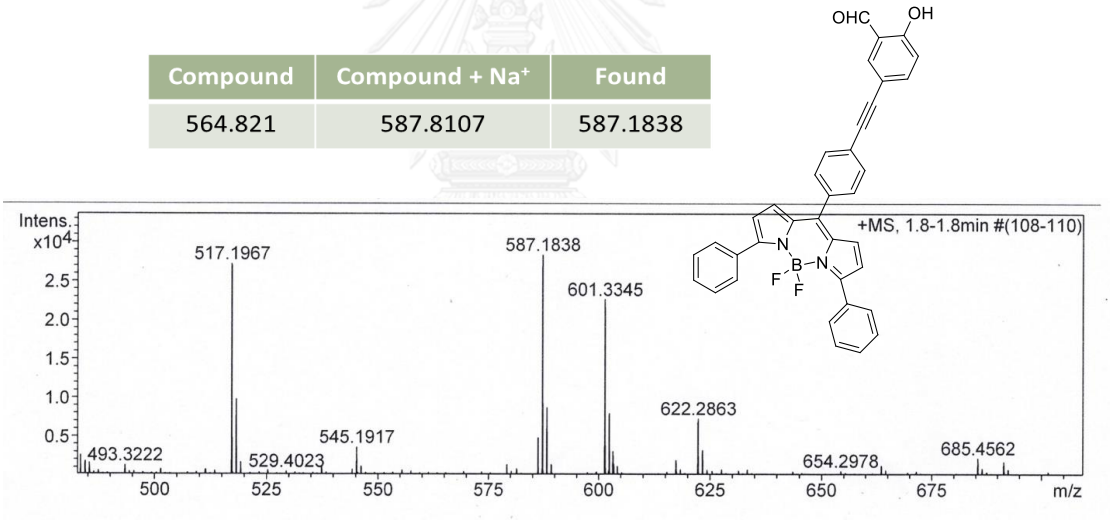

Figure S.14 Mass spectrum of **RSB**

VITA

Mr. Rangsarit Sukato was born in 1988, August 10th at Chonburi province, Thailand. He was finished his high school from Rayongwittayakom at Rayong in 2007. In 2011, he graduated with bachelor's degree in science, major of chemistry from King Mongkut's Institute of Technology Ladkrabang. In 2012, he continues his master's degree of Science in program of Petrochemistry and Polymer Science from Chulalongkorn University. During his master course, he joined Material Advancement and Proficient Synthesis (MAPS) GROUP under supervision of Assist. Prof. Dr. Sumrit Wacharasindhu. His current address is 78 M.6 Bankhai, Bankhai, Rayong, Thailand 21120.